

A numerical study of three catastrophic precipitating events over southern France. I: Numerical framework and synoptic ingredients

O. Nuissier,^{a*} V. Ducrocq,^a D. Ricard,^a C. Lebeaupin^a and S. Anquetin^b

^a CNRM/GMME, Météo-France, Toulouse, France

^b Laboratoire d'étude des Transferts en Hydrologie et Environnement, Grenoble, France

ABSTRACT: This study examines the simulation of three torrential rain events observed on 13–14 October 1995 (the Cévennes case), 12–13 November 1999 (the Aude case) and 8–9 September 2002 (the Gard case) over the southeastern part of France using the Meso-NH non-hydrostatic mesoscale numerical model. These cases were associated with extreme Heavy Precipitation Events (HPEs) with significant precipitation amounts exceeding 500 mm in less than 24 hours. Several sets of numerical experiments were performed with 10 km and 2.5 km horizontal resolutions. In part I of this study, special attention is paid to the experimental design for obtaining realistic simulations of HPEs with the Meso-NH model, as well as the evolution of the synoptic patterns in which the rainfall events are embedded.

The best 2.5 km numerical simulations show the ability of the Meso-NH model to reproduce significant quasi-stationary rainfall events. Moreover, the model fairly reproduces the low-level mesoscale environments associated with the three HPEs. The HPEs formed in a slow-evolving synoptic environment favourable for the development of convective systems (diffluent upper-level southerly flow, PV anomalies, etc.). At lower levels, a southerly to easterly moderate to intense flow provided conditionally unstable and moist air as it moved over the relatively warm Mediterranean Sea, typical for this time of the year (late summer and autumn). The two extreme cases (Gard and Aude) differ from the more classical event (Cévennes) in terms of larger low-level moisture fluxes. Weaker values of conditional convective instability, as in the Aude case, is counterbalanced by a stronger warm and moist low-level jet. The mesoscale triggering and/or sustaining ingredients for deep convection and the physical mechanisms leading to the stationarity of these rainfall events are presented and discussed in a companion paper. Copyright © 2008 Royal Meteorological Society

KEY WORDS mesoscale convective systems; heavy precipitation; non-hydrostatic numerical model

Received 21 August 2006; Revised 2 July 2007; Accepted 17 September 2007

1. Introduction

The western Mediterranean region is prone to devastating flash-flood events, particularly during the autumn. In past decades, devastating flash floods have been responsible for human casualties, and the destruction of houses, buildings, roads, bridges, power and telephone lines, etc. Table I gives a non-exhaustive inventory of dramatic events which have taken place in the Mediterranean area during the last twenty years. All of the coastal areas of the western Mediterranean region are affected (see Figure 1 for geographical locations): southern France with extreme flash-flood events such as those of Vaison-la Romaine (Sénési *et al.*, 1996), Aude (Ducrocq *et al.*, 2003a) and Gard (Ducrocq *et al.*, 2004; Delrieu *et al.*, 2005) on 22 September 1992, 12–13 November 1999 and 8–9 September 2002, respectively; the eastern Spanish coast with, for example, more than 800 mm recorded in 24 hours at Gandia on 3 November 1987 (Llasat

and Puigcerver, 1994; Fernandez *et al.*, 1995; Penarrocha *et al.*, 2002); northwestern Italy (and Sardinia) with the catastrophe of 4–5 November 1994 in the Piedmont region (Buzzi *et al.*, 1998; Doswell *et al.*, 1998; Ferretti *et al.*, 2000; Rotunno and Ferretti, 2001, among others); and even the northern African coast with the most catastrophic event of recent decades in term of human losses in Algiers on 10 November 2001 (Hamadache *et al.*, 2002).

From a climatic point of view, Frei and Schär (1998) have analyzed high-resolution rain-gauge observations of daily surface rainfall to produce a precipitation climatology extending from the Massif Central to the eastern Alps. This climatological study has shown that precipitation is particularly enhanced along the Alpine foothills, with dryer conditions over the mountain ranges. This is one reason which motivated the MAP experiment in this area (Bougeault *et al.*, 2001). However, Frei and Schär (1998) have also clearly shown that the southeastern part of the Massif Central (named Cévennes) is one of the five rainiest areas of the region. Figure 2 focuses on this region of interest and shows the number of days for which

* Correspondence to: Dr O. Nuissier, CNRM/GMME/MICADO, 42 av. G. Coriolis, 31057 Toulouse Cédex, France.
E-mail: olivier.nuissier@meteo.fr

Table I. Summary of recent flash floods around the western Mediterranean.

Place	Date	Surface rainfall (mm)	Human losses	Damage costs (US \$)
Gandia (Spain)	3 Nov 1987	>800 in 24 hours		
Vaison-la Romaine (France)	22 Sep 1992	300 in 24 hours	>50	1 × 10 ⁹
Piedmont region (Italy)	4–5 Nov 1994	300 in 36 hours	>60	12 × 10 ⁹
Aude (France)	12–13 Nov 1999	630 in < 48 hours	>30	3 × 10 ⁶
Algiers (Algeria)	10 Nov 2001	>260 in <24 hours	886	4 × 10 ⁹
Gard (France)	8–9 Sep 2002	>600 in 24 hours	>20	1.5 × 10 ⁹

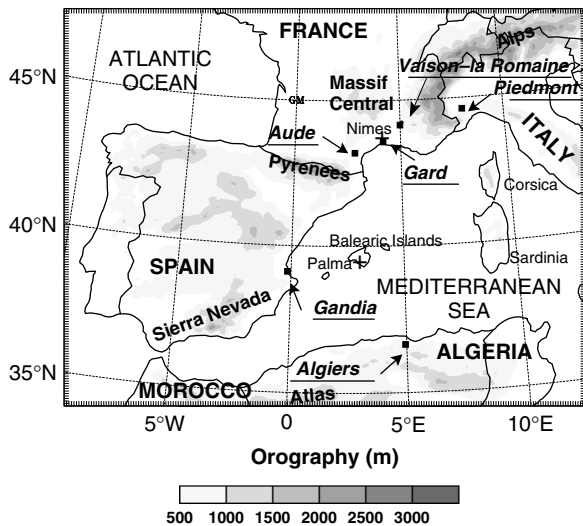


Figure 1. Topography (10 km resolution) of the western Mediterranean region, with the different locations mentioned in the text. The black squares denote a few catastrophic flash-flood events in the area. Crosses show the locations of Nîmes and Palma.

the daily surface rainfall exceeded 200 mm between 1958 and 2004 over southern France; the southern Alps, the

eastern Pyrenees, eastern Corsica and the southern Massif Central are the areas most frequently exposed to heavy precipitation. In other words, it is clear that the heaviest precipitation events occur mainly over the southeastern flanks of the mountainous regions, which are oriented perpendicular to the southerly to easterly moist low-level flow over the Mediterranean Sea.

Heavy precipitation events (HPEs) in the Mediterranean basin can be attributed to either convective or non-convective processes, or a combination of both. Large amounts of precipitation can accumulate over several days when frontal disturbances slow down and are strengthened by the relief of the Massif Central and the Alps, but also significant rainfall totals can be recorded in less than a day (typically more than 200 mm in less than 24 hours, and sometimes in only 6 hours) when a Mesoscale Convective System (MCS) stays over the same area for several hours. Most of the flash-flood events can be attributed to these quasi-stationary MCSs (Riosalido, 1990; Rivrain, 1997; Hernandez *et al.*, 1998; Romero *et al.*, 2000; Ducrocq *et al.*, 2003a, 2004). These convective systems frequently take a characteristic V-shape on infrared satellite images (Scofield, 1985) and are back-building (Bluestein and Jain, 1985). In this process, new

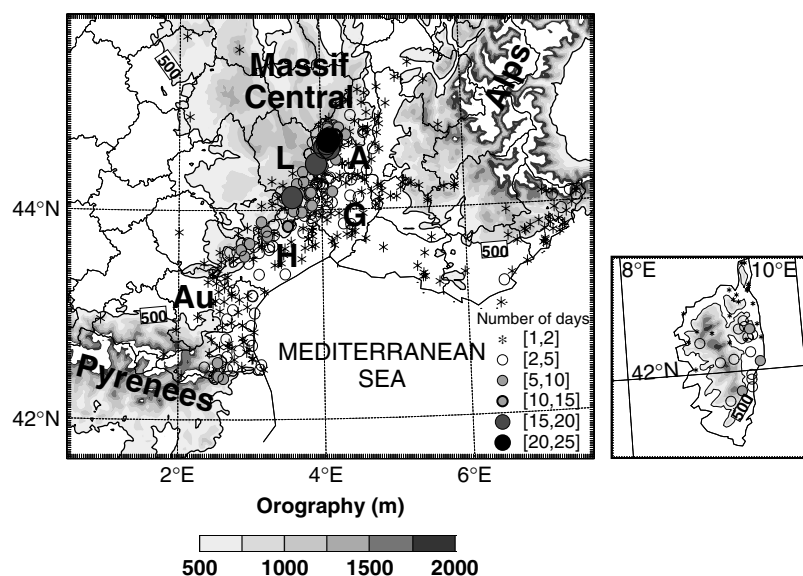


Figure 2. Number of days with daily precipitation greater than 200 mm over southern France from 1958 to 2004. The orography has a bold solid contour at the 500 m level. The thin lines delineate the departments (administrative areas of France); the Aude, Hérault, Gard, Ardèche and Lozère departments are labelled Au, H, G, A and L, respectively. The southeastern region of the Massif Central is named ‘Cévennes’.

convective cells are continuously generated at the V tip, whereas older ones are gradually transported toward the V branches and dissipate downstream. The V-shape cloud pattern results from the interaction of the deep convection and the generally strong southerly to westerly diffluent flow at upper levels. To become stationary, MCSs require triggering mechanisms that release conditional convective instability at the same location over several hours. Quasi-stationary MCSs are particularly efficient in terms of rain production due to their high intensities and their spatial stationarity (Chappell, 1986; Delrieu *et al.*, 2005).

Western Mediterranean regions are favoured locations for major flash floods due to the fact that all the conducive factors for such extreme precipitating events (e.g. discussed by Lin *et al.*, 2001) can be simultaneously observed in the area. The first consists in a relatively warm Mediterranean Sea, which occurs mainly at the end of summer and the beginning of autumn. This feeds in moisture and heats the lowest levels of the troposphere through air–sea sensible and latent-heat fluxes. The second factor is the presence, in most cases, of a strong synoptic-scale trough or a closed cyclone at upper levels, just west of the threat area which generates a southerly to easterly flow that transports the warm and moist air masses from the Mediterranean Sea towards the coast and thus helps to destabilize the air column. The third factor is related to the steep and particular orography of the Mediterranean region which helps to trigger convection within the impinging moist and conditionally unstable low-level flow, but it also channels this very moist low-level jet (LLJ), inducing upwind low-level convergence which contributes to the release of conditional convective instability near the Mediterranean Sea.

The link, even though complex, between heavy precipitation and synoptic-scale troughs and cyclones (and their possible alteration by mountain ranges) has been well established in the past (Doswell *et al.*, 1998; Homar *et al.*, 1999; Massacand *et al.*, 1998). Jansa *et al.* (2001) have found that in most cases (around 90%) of heavy rain in the western Mediterranean, there is a cyclonic centre in the vicinity, usually located so that its presence favours the creation and intensification of the moist low-level flow which feeds the heavy precipitation system. Cyclone intensity could, however, vary from strong and deep systems to weak and shallow depressions, and even in some cases (10%) no cyclone is present in the vicinity.

If it is more or less obvious to clearly identify these synoptic-scale precursors inducing dynamic forcing favourable to torrential event occurrences, one of the most challenging tasks using weather numerical models is to correctly forecast when (and especially where) a MCS will occur and what will be the associated quantitative precipitation. The orography of the western Mediterranean Sea usually interacts with the synoptic flow, modifying the circulation and generating mesoscale disturbances that force and focus the convection in specific areas. For instance, Romero *et al.* (2000) showed that the development of a surface meso-low driven by latent heat release, as well as lee cyclogenesis induced

by the Atlas mountains, could have had a key role in the two severe convective cases they studied. A significant reduction of forecast errors (location, intensity, etc.) associated with Mediterranean HPEs comes through a good representation in numerical models of both the synoptic- and mesoscale ingredients, in addition to a description of terrain conditions which are likely to influence these meteorological phenomena.

As shown by Figure 2, the southeastern region of France is often affected by intense flash-flooding episodes. The goal of these two papers is therefore to analyze and document three HPEs observed over this specific region. Two of them are extreme flash-flood events with significant precipitation totals (more than 500 mm in less than 24 hours), whereas the third had its precipitation maximum placed over the region statistically most exposed to HPEs, e.g. along the Massif Central southeastern flank (Cévennes region). Even though many studies have focused on the way in which synoptic-scale conditions and terrain characteristics are conducive (or not) for triggering heavy precipitation, it is important to identify the mechanisms that lead to the formation, distribution and especially persistence over several hours of this kind of precipitation at a specific location. The main goal of our study is to use realistic structures and evolutions of three representative HPEs simulated by a convective-scale model to highlight the factors leading to the stationarity of the heavy precipitation systems which are responsible for accumulation of large rainfall amounts over southeastern France. In part I of this study, greater attention is paid to the experimental design needed to obtain realistic simulations of HPEs together with the evolution of the synoptic patterns in which the rainfall events are embedded, whereas the mesoscale and fine-scale structures of the MCSs and their environment, as well as the role of the convection and orography, are discussed in a companion paper (Ducrocq *et al.*, 2008).

Following this introduction, an overview of the meteorological phenomena is provided. The description of the experimental design is outlined in Section 3, followed by an overview of the results of the simulations in Section 4. Section 5 discusses the evolution of the synoptic patterns in which the precipitating systems are embedded. Finally, concluding remarks are presented in the last section.

2. The case-studies

Our study focuses on three flood events: 13–14 October 1995 (the Cévennes case), 8–9 September 2002 (the Gard case) and 12–13 November 1999 (the Aude case). The Cévennes and Gard cases occurred in the vicinity of the Massif Central, in the Ardèche and Gard departments, respectively, whereas the Aude event took place in the Aude region between the Massif Central and the eastern Pyrenees. For all three cases, most of the precipitation was induced by a quasi-stationary MCS. Although the rainfall events are described in Ducrocq *et al.* (2002, 2003a, 2004) and Delrieu *et al.* (2005), this present

section provides a detailed overview of the life cycle of the different systems adopting a uniform presentation for the three cases.

2.1. Cévennes case

During the morning of 13 October 1995, a moist sea-air intrusion over the Hérault and Gard departments led to nearly saturated low levels over these regions. Convective activity started around 1800 UTC on 13 October when a first MCS formed offshore. This first system (labelled MCS 1 in Figure 3(a)) contributed to the moistening of the southerly low-level flow, thus enhancing further the moisture over the region and leading to conducive conditions for the development of another MCS (labeled MCS 2 in Figure 3(a)) during the evening over the Massif Central foothills. After 2100 UTC, several convective cells formed over the sea and the Gard department and then progressed northwards while strengthening, finally merging into a single system at 2230 UTC (MCS 2). Radar images (not shown) indicate that MCS 2 was continually fed by a train of convective cells advected toward the mountainous region of Massif Central by the southerly flow. MCS 2 stayed over the Gard, Ardèche and Lozère departments for about 9 hours before moving northeastwards around 0800 UTC on 14 October while decaying (as indicated by warmer cloud tops in Figure 3(c)). At its mature stage around 0200 UTC, the cloud pattern of the MCS formed a typical V-shape on the infrared imagery, with the coldest top cloud extending between the Gard and Lozère departments (Figure 3(b)).

Figure 4(a) shows the rain amounts recorded by Météo-France's rain-gauge network for the Cévennes case from 2100 UTC on 13 October to 0800 UTC on 14 October. The heavy precipitation for that case mainly occurred along the Massif Central southeastern foothills with a peak of precipitation of about 262 mm over the northwestern portion of the Gard department. Such an accumulated rainfall distribution is typical of flash-flooding episodes over the region. Maximum precipitation was recorded over the Gardon d'Anduze river watershed, an area of about 545 km². The maximum specific discharge recorded at the outlet of this catchment was about 2.6 m³ s⁻¹ km⁻² at 0700 UTC on 14 October, whereas the maximum hourly precipitation was recorded around midnight (Figure 4(b)). Fortunately, little damage was observed in the region and no casualties were reported for this Cévennes case.

2.2. Gard case

The first convective cells associated with Gard event appeared over the Mediterranean Sea around 0400 UTC on 8 September 2002, in the warm air well ahead of the surface front that affected western France at that time. Progressing northwards, the convection started to organize while forming a MCS just south of the Gard

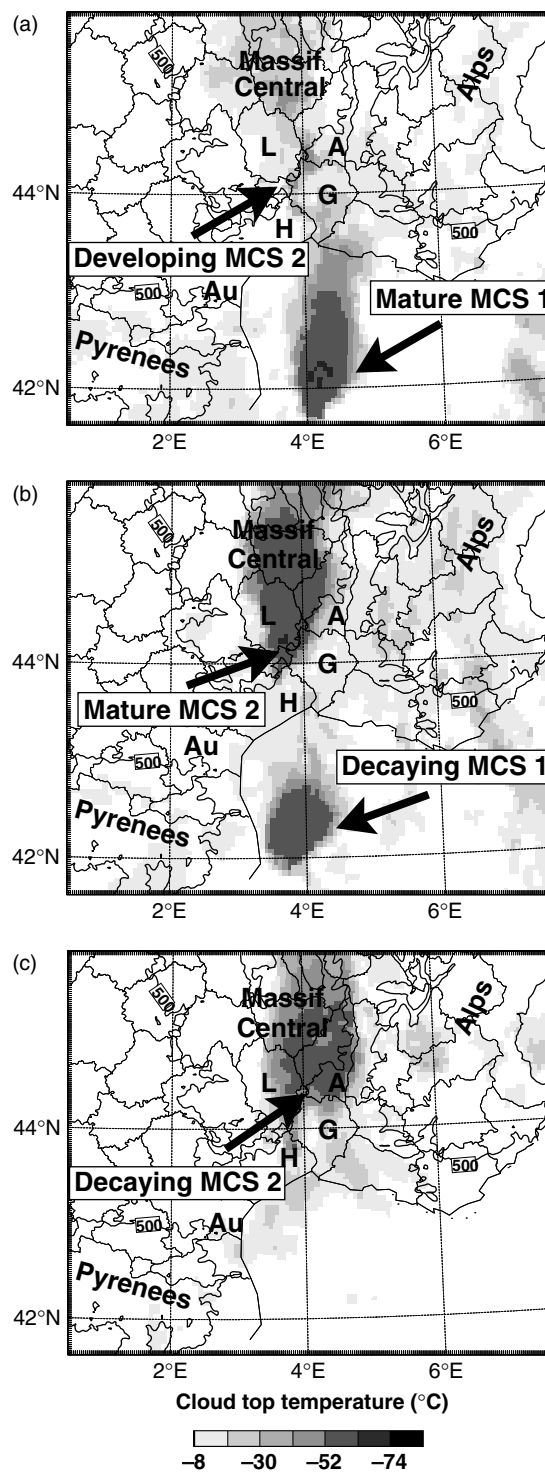


Figure 3. METEOSAT infrared brightness temperature for the Cévennes case at (a) the growing stage (21 UTC, 13 October 1995), (b) the mature stage (02 UTC, 14 October) and (c) the decaying stage (08 UTC, 14 October). The bold contour shows the 500 m level. The Au, H, G, A and L labels are as in Figure 2.

department from 0800 UTC as shown by the radar reflectivity over the region (Figure 5(a)). The convective system stayed over almost the same region from 1200 UTC on 8 September until 1200 UTC on 9 September. During its mature stage, the cloud shield took on a classical V-shape on the infrared images, with the tip of the

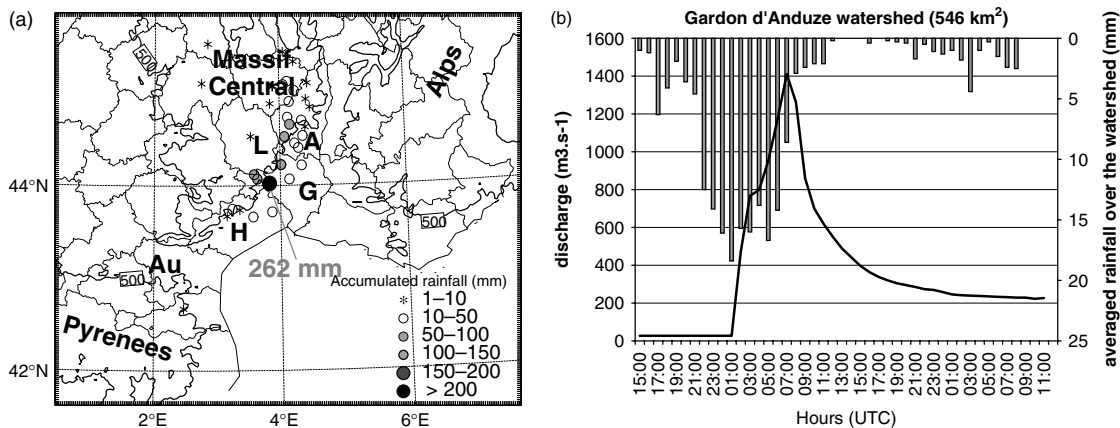


Figure 4. (a) Accumulated precipitation (mm) from Météo-France's rain-gauge network for the Cévennes case from 21 UTC, 13 October to 08 UTC, 14 October 1995. The bold contour shows the 500 m level. (b) Rainfall (grey bars) and discharge (solid curve) over the Gardon d'Anduze watershed.

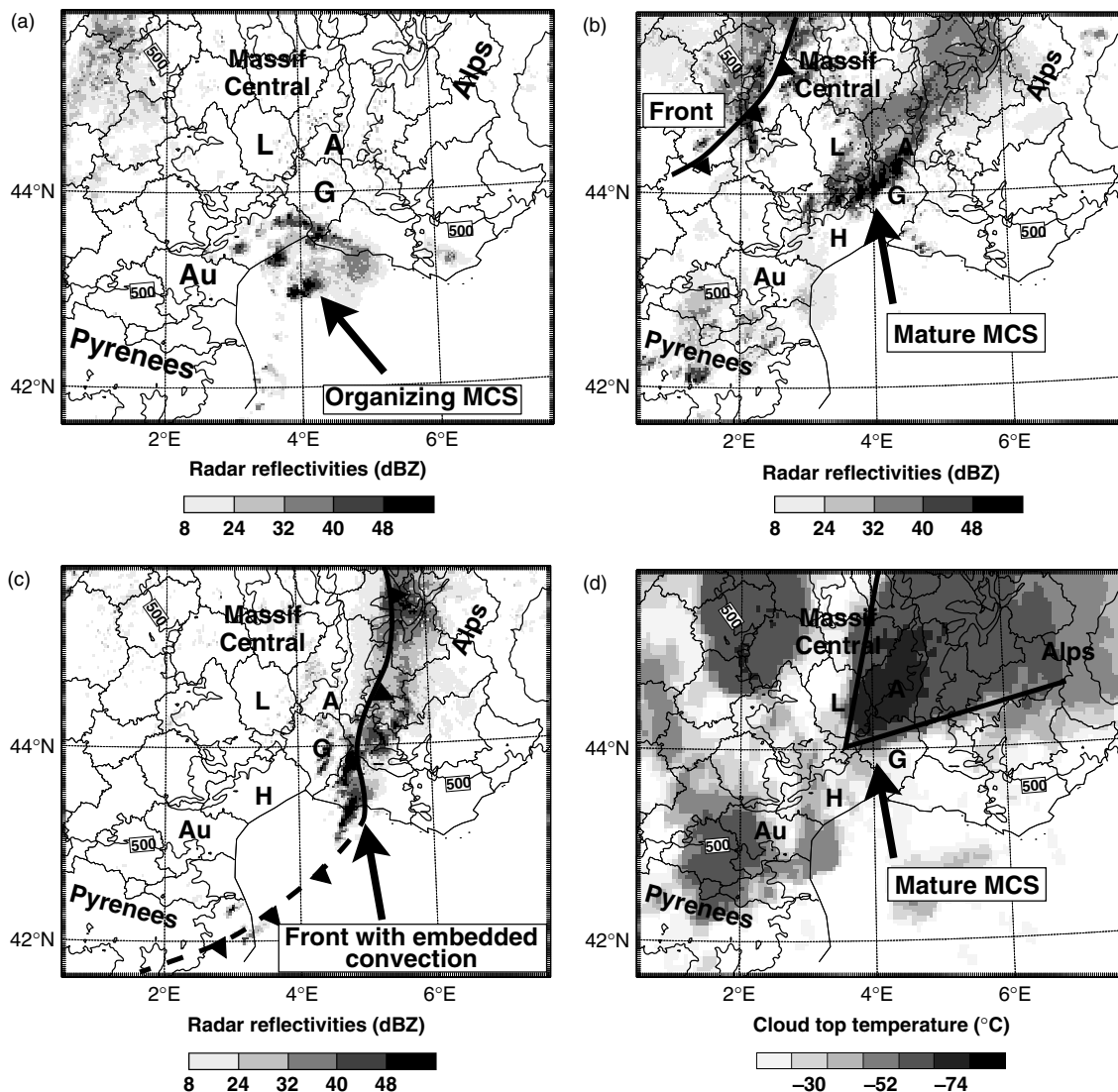


Figure 5. Composite radar reflectivities from the observations of the Gard case at (a) the growing stage (08 UTC, 8 September 2002), (b) the mature stage (2230 UTC, 8 September) and (c) the decaying stage (12 UTC, 9 September). (d) is as (b) but for METEOSAT infrared brightness temperature. The bold solid and solid/dashed lines in (b) and (c) denote the surface front (undulating in (c)). Au, H, G, A and L labels are as in Figure 2.

V facing the upper-level southwesterly flow that prevailed at that time (Figure 5(d)). Beneath the cloud shield, the convective precipitation mainly affected the Gard region (as indicated in Figure 5(b)), while the stratiform precipitation was extending farther to the north. At this time, the MCS took a southwest–northeast orientation according to the prevailing mid- to upper-level tropospheric flow. But as the upper-level trough axis tilted counterclockwise in a northwest–southeast orientation later on the night of 8 September, the convective system moved in a more north–south orientation and began a slow northwestward motion. Early in the morning of 9 September, the surface cold front approached from the west and merged with the MCS around 0400 UTC. As the cold front was progressing eastwards, the whole precipitating system again swept over the Gard department during the late morning of 9 September (Figure 5(c)).

The Gard precipitation event was an exceptional one due to many factors. Firstly, Figure 6 shows that the intensity of the event was extreme with maximum precipitation around 600–700 mm in 24 hours (from 1200 UTC on 8 September) near Alès. Secondly, the area affected by precipitation over 200 mm was considerable. This area extended over at least 3000 km² covering a large portion of the northern Gard department, as far as the Massif Central foothills in Ardèche. As emphasized by Delrieu *et al.* (2005), the episode underwent three distinct phases. In phase 1 from 0800 UTC till 2200 UTC on 8 September, the MCS developed and became stationary. The heaviest precipitation was located over the plains just north of the city of Nîmes (Gard department), i.e. a rather unusual location according to the heavy rainfall climatology (Figure 2). Maximum rainfall amounts were about 300 mm during this phase. Between 2200 UTC and 0400 UTC (phase 2), the system slowly moved northwestwards. The MCS produced rainfall amounts greater than 100 mm over this 6-hour period. Finally, after 0400 UTC (phase 3), the surface cold front approached and

swept over the region again producing sustained showers with rainfall amounts exceeding 100 mm during an 8-hour period.

The river discharges in the region were also exceptional. For the Gard and Vidourle river watersheds, peak discharges twice as high as the 10-year return period discharge were recorded (Delrieu *et al.* 2005; Chancibault *et al.*, 2006). The estimated peak discharges of the upstream watersheds of these rivers were very high (5–10 m³s⁻¹km⁻²), locally reaching extreme values as high as 20 m³s⁻¹km⁻². Such large discharge measurements can be explained by both the spatial extent and the intensity of the heavy rainfall. This event caused damage estimated to be 1.2 billion US dollars (Huet *et al.*, 2003) and led to the deaths of 25 people (Table I).

2.3. Aude case

In the early afternoon of 12 November 1999, the first convective cells formed a few tens of kilometers east of the Aude coast. This area of intense precipitation (Figure 7(a)) gradually moved westwards while strengthening. Convection organized and evolved to a MCS which stayed stationary over the Aude department from 1600 UTC on 12 November until 0000 UTC on 13 November. Similar to the Cévennes and Gard cases, this system took a classical V-shape as shown on the infrared imagery in Figure 7(d), resulting from the intense diffluent flow aloft. However, beneath the upper-level cloud plume, the precipitation was organized in a narrow line with an approximate north–south orientation (Figure 7(b)). Between 0000 and 0400 UTC on 13 November, other strong convective cells coming from the Balearic Islands merged with the previous MCS. The stormy activity started to decrease after 0400 UTC as the system moved off the Aude coast while becoming less organized (Figure 7(c)).

During the Aude event, high surface rainfall amounts were recorded which in large part can be directly

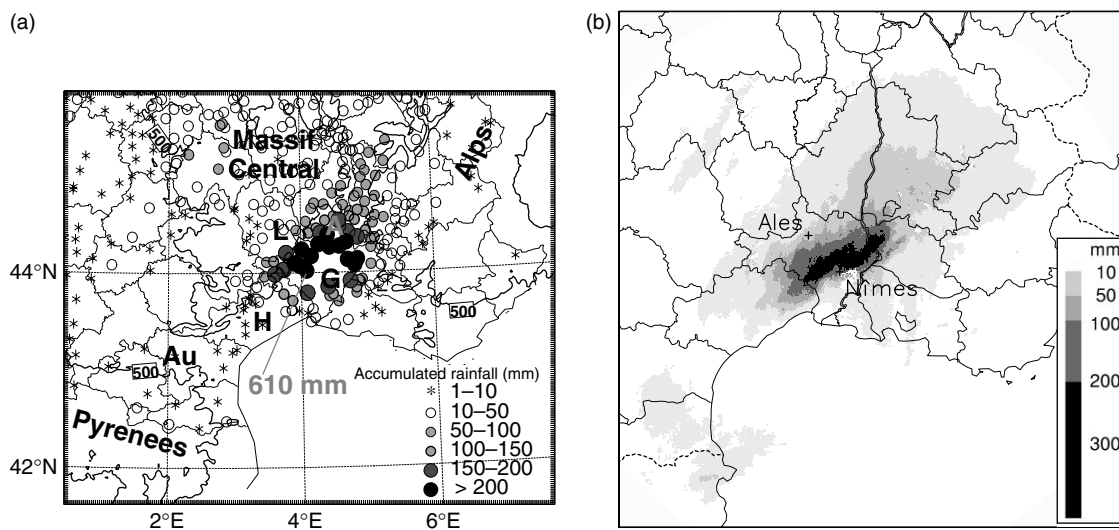


Figure 6. (a) Accumulated precipitation (mm) from Météo-France's rain-gauge network for the Gard case from 12 UTC, 8 September to 12 UTC, 9 September 2002. (b) shows the accumulated rainfall from the Nîmes radar for the same period.

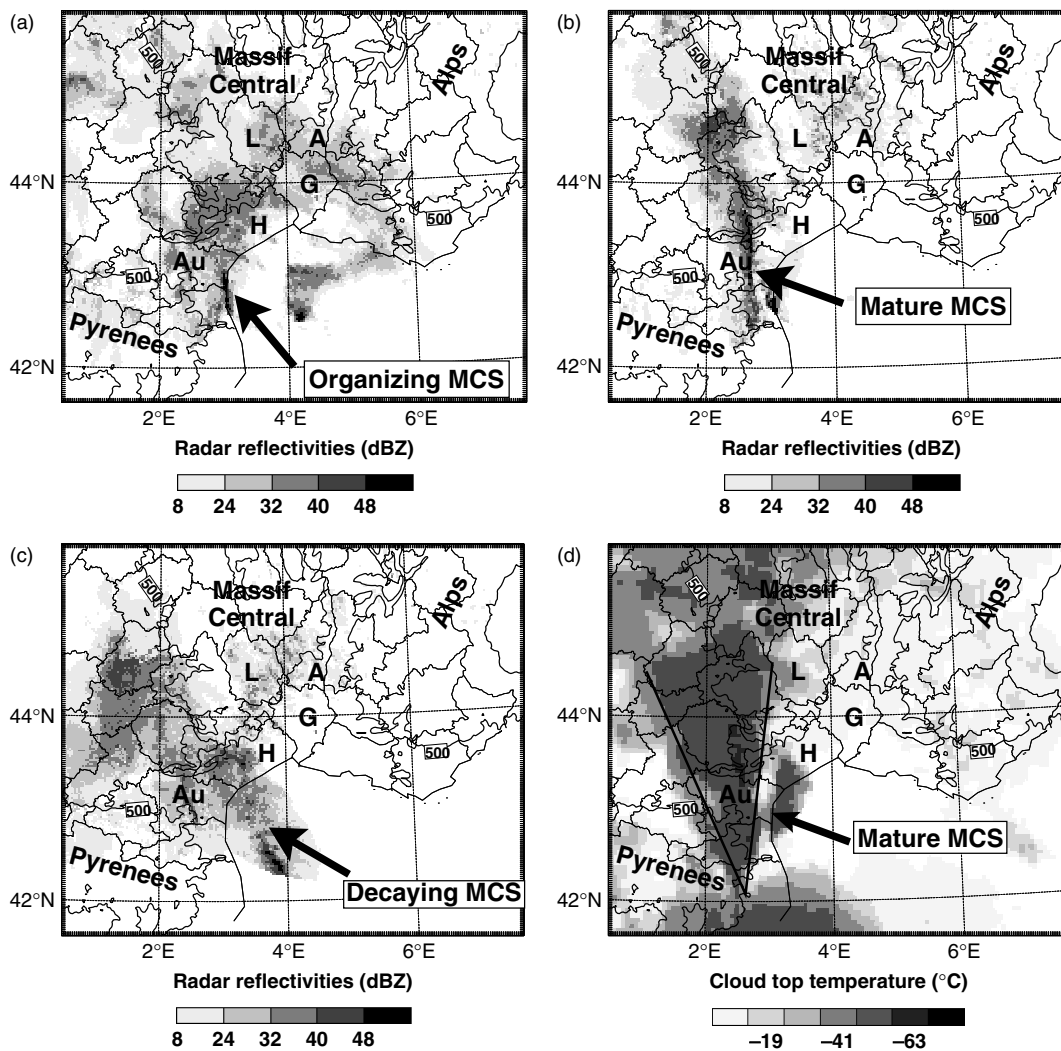


Figure 7. As Figure 5, but for the Aude case. Times are (a) 16 UTC, 12 November 1999, (b) 00 UTC, 13 November and (c) 04 UTC, 13 November. (d) is as (b) but for METEOSAT infrared brightness temperature.

attributed to the MCS mentioned above. Figure 8 shows that from 1200 UTC on 12 November until 0600 UTC the next day, 485 mm fell at Lézignan-Corbières in the Aude department. The Aude event had some strong similarities with the Gard case in terms of the spatial extent of the accumulated surface rainfall. Indeed, the area receiving more than 200 mm in 48 hours extended more than 150 km in length and about 50 km in width. This extreme rainfall event resulted in one of the century's most significant floods in the Aude region and produced remarkable flash floods in some catchments. Peak flood discharge as high as $10 \text{ m}^3 \text{ s}^{-1} \text{ km}^{-2}$ were recorded from the small upstream watersheds (areas $< 100 \text{ km}^2$) of the Aude river (Gaume *et al.*, 2004). Strong low-level easterly winds were also recorded during this event. Surface wind gusts reached about $35\text{--}40 \text{ m s}^{-1}$ during the morning of 12 November, and these high winds along the coast lasted at least 24 hours causing a significant surge of 4–5 feet above normal tide levels. This prevented the rivers from discharging into the

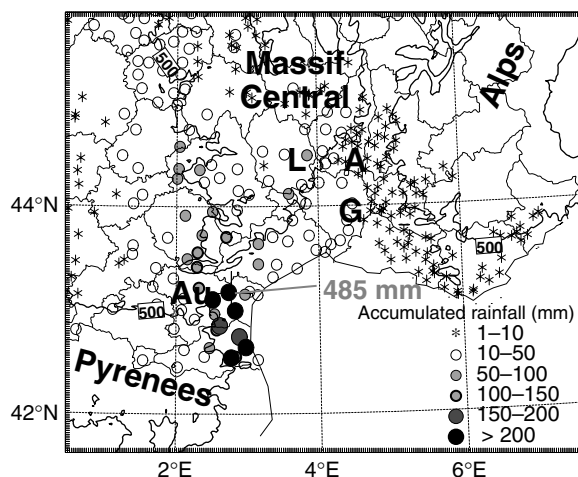


Figure 8. As Figure 4, but for the Aude case from 12 UTC, 12 November 1999 to 06 UTC, 13 November.

Mediterranean Sea, thereby aggravating the flooding. This flash-flood event was particularly deadly, resulting in the deaths of 36 people (Table I).

3. Description of the numerical experiments

3.1. The Meso-NH model

A three-dimensional version of the French Meso-NH non-hydrostatic mesoscale numerical model (Lafore *et al.*, 1998) has been used for the simulation of the precipitating events. Meso-NH allows the simultaneous use of several nested grids in a two-way interactive mode (Clark and Farley, 1984; Stein *et al.*, 2000); the coarser grid provides the lateral boundary conditions to the finer grid, while the variables of the coarser grid are relaxed with a short relaxation time toward the finer grid's values in the overlapping area. For this study, the domain configuration has been retained which was used with success by Ducrocq *et al.* (2002) and Ricard (2005) for quantitative precipitation forecasting, by Chancibault *et al.* (2006) for hydrological response, by Brenot *et al.* (2006) based on ground GPS observations, and by Caumont *et al.* (2006) based on radar reflectivity, i.e. two two-way nested domains in the horizontal plane with horizontal grid spacings of about 10 and 2.5 km, with the 2.5 km domains ranging from 250×375 km to 600×600 km. The Gal-Chen and Sommerville (1975) vertical coordinate is used for 40 vertical levels; the spacing between them varies continuously with altitude, from 75 m close to the surface to 900 m aloft. The top of the domain is at 19 km altitude, and Rayleigh damping is progressively applied above 15 km altitude (i.e. the last six levels) to the perturbations of the wind components and the thermodynamical variables with respect to their large-scale values, in order to prevent spurious reflections from the upper boundary.

The prognostic variables are the three Cartesian components of velocity, the dry potential temperature, the different water mixing ratios and the turbulent kinetic energy. Pressure perturbations are determined by solving the elliptic equation obtained by combining air mass continuity and momentum conservation equations. A bulk microphysical scheme (Caniaux *et al.* 1994; Pinty and Jabouille 1998) governs the equations of the six water species: water vapour, cloud water, rain water, primary ice, snow aggregates, and graupel. Moreover, for the coarser horizontal resolutions (>10 km), the subgrid-scale convection is parametrized by the Kain and Fritsch (1990, 1993) scheme, adapted to the Meso-NH model by Bechtold *et al.* (2001). The turbulence parametrization is based on a 1.5-order closure (Cuxart *et al.*, 2000). For the coarser grids, the mixing length follows the method

of Bougeault and Lacarrère (1989) and the horizontal gradients are not considered. For the finer grids, the mixing length is directly proportional to the grid volume and three-dimensional turbulent fluxes are modelled (Redelsperger and Sommeria, 1981).

3.2. Experimental design

The different numerical experiments performed for each case are summarized in Table II. In order to document the larger-scale environment, a first set of simulations was performed with only the 10 km resolution domain (REF10 experiments in Table II). The initial conditions are provided by the large-scale operational analysis of the French ARPEGE NWP suite at noon. Additional simulations (not listed in Table II) were performed to test the model sensitivity to the time of the initial conditions, with the runs starting 12 hours earlier than the REF10 simulations.

In order to study the finer-scale ingredients, Meso-NH was run at about a 2.5 km resolution in order to have an explicit treatment of the convection. The REF2.5 experiments consider the same initial conditions as the REF10, but with the two interactive domains at 10 km and 2.5 km resolutions. However, in the Cévennes and Gard cases, the REF2.5 experiments failed to reproduce the key characteristics of the phenomena, so other initial conditions were investigated and tested. A Mesoscale Data Analysis (MDA) following Ducrocq *et al.* (2000, hereafter D00) was therefore used to obtain initial conditions for the MDA experiments. The fine-scale initialization procedure of D00 was applied to these two cases after the observed triggering of the convection, to take into account of the early stage of convective activity in the analysis. First, mesonet surface observations are included both in the altitude and surface optimal interpolation analyses of the Aladin model to provide the initial states of both the 10 km and 2.5 km domain. Then, a cloud and precipitation analysis, based on the radar reflectivities and Meteosat infrared brightness temperatures, drove a moisture and microphysical adjustment that was finally superimposed on the initial state of the 2.5 km domain. The adjustment is such that the vapour mixing ratio inside the cloudy areas is set to its saturated value with respect to the ambient temperature. Also, some rainwater (snow) is inserted inside the rainy areas below (above) the freezing level. (D00 provides a more complete description of this fine-scale initialization procedure.)

Table II. Initial conditions used for the simulation of different cases.

Case	REF10	REF2.5	MDA
	1 domain (10 km) from ARPEGE analysis	2 domains (10 and 2.5 km) from ARPEGE analysis	2 domains (10 and 2.5 km) from D00's full mesoscale initialization technique
Cévennes	1200 → 1200 UTC	1200 → 0600 UTC	2200 → 1200 UTC
Gard	1200 → 1200 UTC	1200 → 1200 UTC	1200 → 1200 UTC
Aude	1200 → 1200 UTC	1200 → 0600 UTC	

In order to highlight the mesoscale forcing, additional orography and microphysical parametrization sensitivity experiments were performed. The sensitivity experiments are presented in the companion paper.

4. Overview of the simulations

Chancibault *et al.* (2006) have assessed the validity of the high-resolution simulations of the Gard case by simulating stream flow with the topography-based model TOPMODEL (Beven and Kirkby, 1979; Beven *et al.*, 1995) driven by Meso-NH model rainfall. They found that, for the Gard case, the MDA simulations produced more realistic peak flows, which were higher than those obtained for REF2.5 experiments. Furthermore, Ducrocq *et al.* (2002) calculated various scores to assess the high-resolution rainfall numerical forecasts for the Cévennes and Aude cases. They concluded that while the increase in resolution significantly improves the results for the Aude case (REF2.5), it was necessary to apply the MDA procedure to get a more realistic rainfall event for the Cévennes case. The best simulations at 2.5 km resolution (i.e. MDA for Cévennes and Gard cases, REF2.5 for the Aude case) identified by these previous studies are here further compared against observations to corroborate that realistic simulations of the HPEs and of their low-level mesoscale environment have been obtained and could be used to study the events which are described in the following sub-sections. As the 10 km simulations are used to characterize the evolution of the synoptic-scale environment in the following, they are also verified against the ARPEGE large-scale analyses.

4.1. Cévennes case

4.1.1. Upper-level synoptic-scale environment forecast

The upper-level synoptic situation is presented in Figure 9(a) at the initial time of REF10 for the Cévennes case (i.e. at 1200 UTC on 13 October 1995). The synoptic situation was characterized by a large upper-level cold low located well away from France (between 20 and 25°W) and by a mid- to upper-level ridge centred over central Europe. Between both these large-scale structures prevailed a fair upper-level southerly flow and the associated height gradients were rather weak. Analysis of the surface pressure (not shown) reveals that anticyclonic conditions dominated over most of the convective area. Although the signal of synoptic forcing is not obvious in the Cévennes event, one can note the presence of a short-wave trough located near the Algerian coast, associated with a decreasing dynamic tropopause altitude. The dynamic tropopause height is estimated using the 1.5 PVU (Potential Vorticity Unit) surface. The low elevation of this surface indicates a stratospheric air intrusion into the troposphere, generally associated with decreasing pressure at upper levels. This configuration,

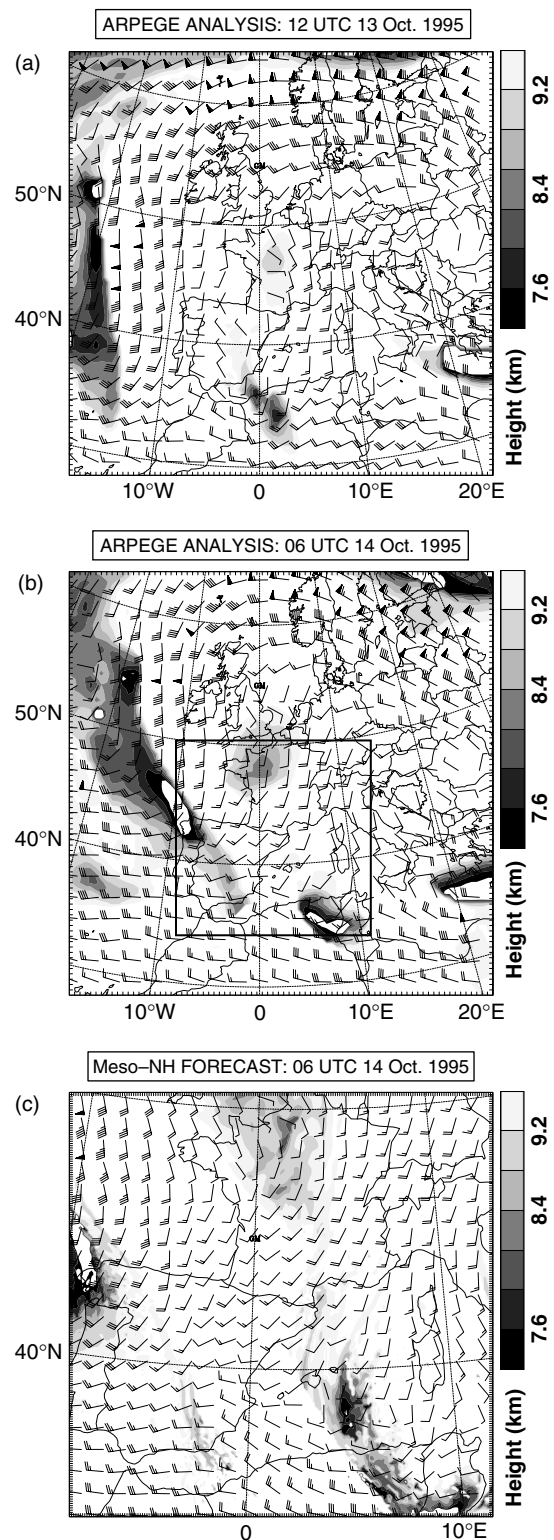


Figure 9. 500 hPa winds (barbs) and 1.5 PVU surface height (shading) for the Cévennes case: (a) and (b) are from the ARPEGE analysis and (c) is from REF10.

in addition to cold air aloft (not shown), helped to destabilize the air mass over the Mediterranean Sea.

After 12 hours of simulation (at 0600 UTC on 14 October), the Meso-NH model simulated the slow evolution of the synoptic pattern fairly well (Figure 9(c) versus 9(b)).

Indeed, coming from a southerly then from a southwesterly direction, the upper-level flow was still weak in the area of interest and the small short-wave trough depicted at 1200 UTC on 13 October moved very slightly eastwards. Moreover, persistence of a mid- to upper-level ridge, centred over the north of Italy and central Europe is another factor at the synoptic scale which explains the slow evolution of the synoptic pattern. Moreover, the upper-level ridge which stalled over central Europe also increased the amplitude of the upper-level trough which, in turn, may have acted to increase upper-level divergence over southern France.

4.1.2. Low-level mesoscale environment forecast

It is also important to validate the simulation of the location and the strength of the low-level inflow. Figure 10(a) and (c) show the 2 m above ground level (AGL) simulated temperature and wind for the best 2.5 km simulation at 0300 UTC on 14 October 1995 for the Cévennes case. The highest surface temperatures ($\approx 20^\circ\text{C}$) are co-located with the LLJ and reach the coast just south of the Hérault department, in good agreement with the observations (Figure 10(b) and (d)). The best simulation also reproduces quite well a moderate south to southeasterly low-level flow impinging upon the Massif Central foothills.

4.1.3. Heavy precipitation forecast

For the Cévennes case, the simulated MCS presents itself as a southwest–northeast elongated precipitating line oriented along the Massif Central, as illustrated by the simulated radar reflectivities (Figure 11(a)). For this case, the maximum simulated radar echoes (≈ 45 dBZ) seem to be generated and focused over a limited area of the Massif Central foothills (not exceeding 1400 km^2), but in a region typified by heavy precipitation (Figure 2). The model succeeds in simulating the whole life cycle of the MCS, including its decaying phase.

The observed surface rainfall for this case (Figure 11(b)) consists of an area of marked rainfall (with a peak of 176 mm in only 6 hours), extending from the Hérault to the Ardèche departments. Although the maximum simulated rainfall is underestimated (about 108 mm), the best simulation predicts both the pattern and the amounts quite well (Figure 11(d)). Also, the simulated surface rainfall in the best simulation is considerably improved over the REF10, as Meso-NH simulates a maximum rainfall amount of only 28 mm, well south of the observed location (Figure 11(c)). Furthermore, the model provides a good representation of the stationarity of the simulated precipitation event. The rainfall time series shown in Figure 12 depicts a well-defined rainfall peak with a maximum 1-hour accumulated rainfall of

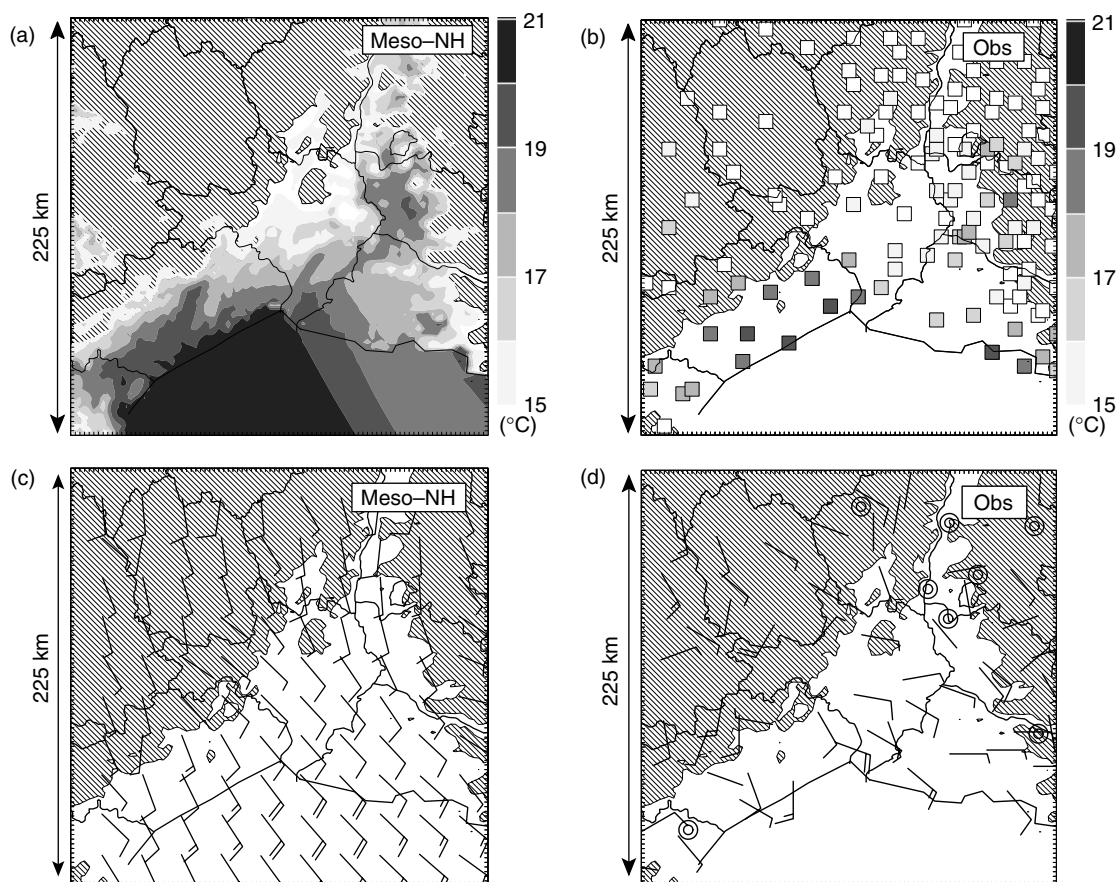


Figure 10. (a) 2 m AGL temperature (shading) and (c) 10 m AGL wind (barbs) for the Cévennes case from the MDA simulation at 0300 UTC, 14 October 1995. (b) and (d) show the corresponding observations at the same time. Orography above 250 m is shown hatched.

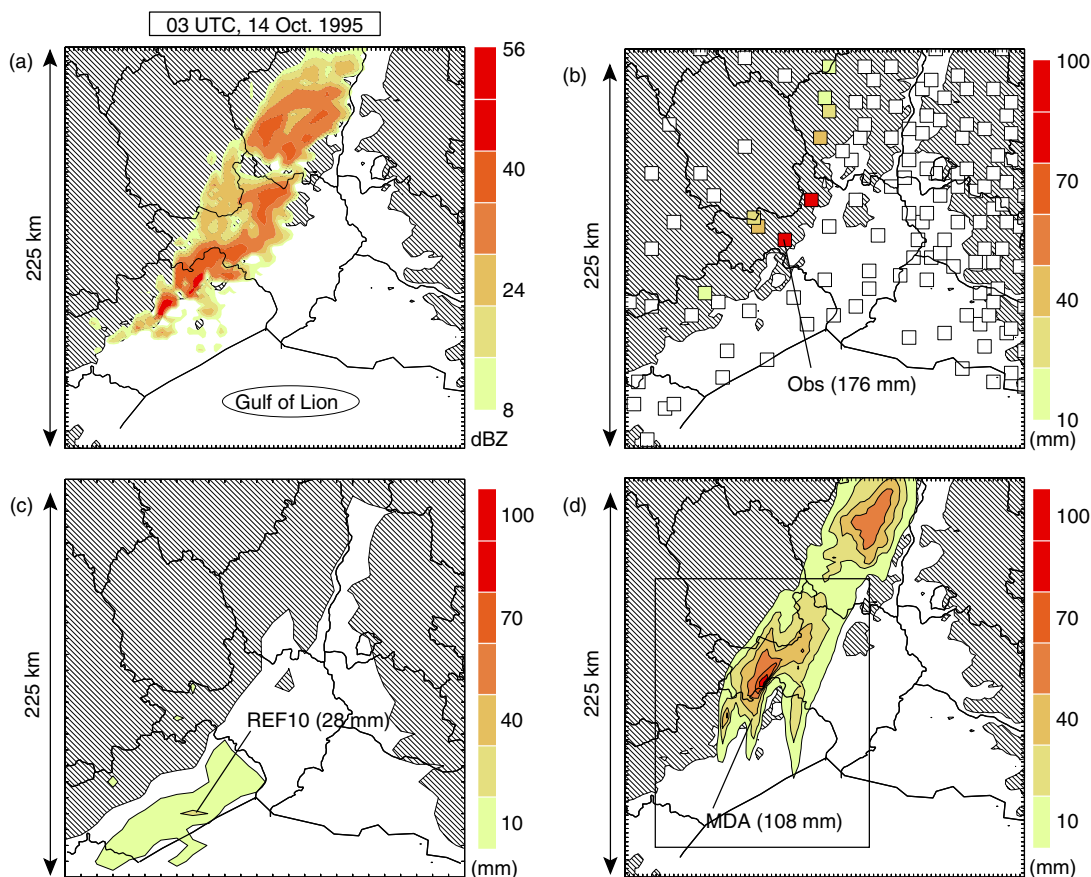


Figure 11. (a) Simulated radar reflectivities (shading) at 2 km altitude from the MDA for the Cévennes case. (b) rainfall observations from 00 to 06 UTC, 14 October 1995. (c) and (d) show the simulated accumulated rainfall (shading) over the model domain for the REF10 experiment and MDA, respectively. Hatching shows orography above 250 m. This figure is available in colour online at www.interscience.wiley.com/qj

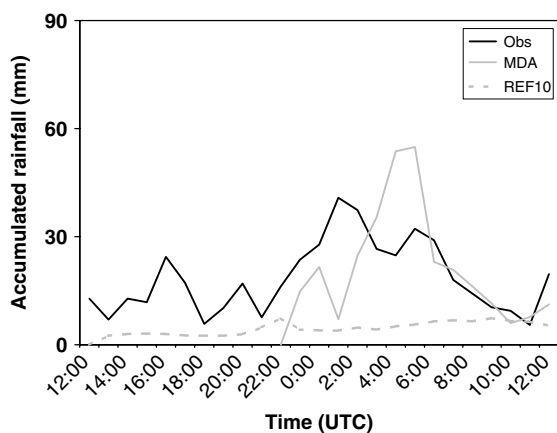


Figure 12. Maximum 1-hour accumulated precipitation for the Cévennes case in the box shown in Figure 11(d) from the REF10 (dashed grey) and MDA (solid grey) simulations and observations (solid black).

about 55 mm for the best simulation, against only 7 mm in the REF10 experiment simulation.

4.2. Gard case

4.2.1. Upper-level synoptic-scale environment forecast

At 1200 UTC on 8 September 2002, the meteorological situation was dominated by an upper-level cold low

centred over Ireland extending via a trough toward the Iberian Peninsula (Figure 13(a)). The trough axis, with a roughly northnortheast–southsouthwest orientation, was generating a southwesterly diffluent flow of about 20 m s^{-1} over southeastern France. Thus, contrary to the Cévennes case, the upper-level circulation was significantly more dynamic and stronger synoptic forcing prevailed for this event. Figure 13(a) also shows the presence of several PV anomalies circulating around the trough axis. Such conditions were precursors for enhancing the upper-level divergent flow over southeastern France which provided additional upward motion for convective triggering. At 0000 UTC on 9 September, the 500 hPa flow for REF10 indicated that the trough axis tilted more northwest–southeast and moved closer to France (Figure 13(b)). The upper-level flow strengthened to around 30 m s^{-1} , but the flow kept its general southwest component and its diffluent feature. As with the Cévennes case, the Meso-NH model succeeded in simulating a slow evolution of the synoptic pattern conducive to heavy precipitation (Figure 13(b) versus Figure 13(c)).

4.2.2. Low-level mesoscale environment forecast

Simulated 2 m AGL temperature and 10 m wind for the Gard case at 1800 UTC on 8 September 2002 are shown in Figure 14 for the best 2.5 km simulation. The observations, as well as the best simulation, depict a warm south

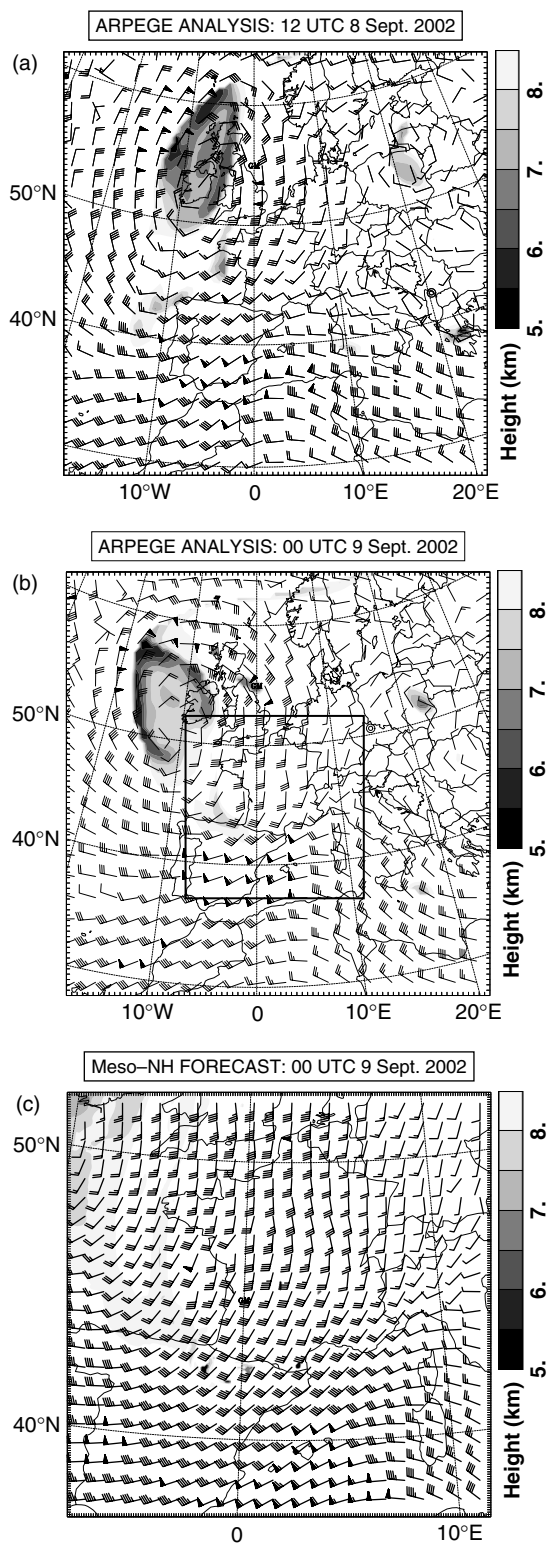


Figure 13. As Figure 9, but for the Gard case.

to southeasterly low-level flow of about 10 m s^{-1} coming from the Mediterranean Sea. An interesting feature which is well simulated by the model is the stronger meridional surface temperature of 5–6 K just south of Gard, marking the boundary between the warm and moist low-level flow and the cold surface air mass generated beneath the precipitation system.

4.2.3. Heavy precipitation forecast

The simulated IR brightness temperature is shown in Figure 15. The simulated MCS for the Gard case is quite impressive, as the associated cloud shield extends over at least six departments (i.e. about $16\,000 \text{ km}^2$). The precipitating structure of the system shows a strong convective part anchored over the flooded location and a less intense stratiform region extending downstream (Figure 16(a)). However the most intense radar reflectivities (i.e. $>45 \text{ dBZ}$) are located in an unusual area over the central plains of Gard, which means well upstream of the Cévennes case (Figure 16(a) versus Figure 11(a)). Also, Figure 15 displays a very realistic signature of the interaction between the deep convection and the strong southwesterly flow aloft, which is about 35 m s^{-1} (not shown). The cloud shield has the classical V-shape in the simulated infrared imagery as in the observed METEOSAT imagery (Figure 5(d)).

Accumulated precipitation from the simulations are shown in Figure 16. Whereas the model starting from the ARPEGE large-scale analysis with low resolution (Figure 16c) did not succeed in simulating realistic rainfall amounts at the correct locations, the best simulation (Figure 16(d)) gives much better results with a simulated rainfall peaking at about 250 mm just over the central plains of Gard, in good agreement with the observations (Figure 16(b)). In contrast to the Cévennes case, for which heaviest precipitation and windward foothills were co-located, the Gard case is marked by an unusual location of maximum precipitation, well upstream of the first Massif Central foothills. The first phase (up to 22 UTC, 8 Sept. 2002) of the event is particularly well reproduced. Although an intense 1-hour accumulated surface rainfall of about 50 mm is predicted by the model (Figure 17), the simulated convective system is located too far north in the second and third phases of the event. (A detailed hydrological evaluation of this simulation can be found in Chancibault *et al.*, 2006). The following discussions of the best simulations for this specific Gard case will therefore be focused on the first phase of the event.

4.3. Aude case

4.3.1. Upper-level synoptic-scale environment forecast

Similar to the Gard case, the Aude event also exhibits a strong dynamic circulation and obvious upper-level forcing. At 12 UTC on 12 November 1999, a pronounced and elongated upper-level deep tropospheric trough was centred over northwestern Spain (Figure 18(a)). This pattern generated a broad and fast southerly flow over the Mediterranean Sea, from the north African coast to France. Even though the meteorological context in the Aude case seems to be characterized by a dynamic upper-level circulation similar to the Gard case, the synoptic forcing tended to be stronger, similar to those described by Maddox *et al.* (1979) and Chappell (1986). The upper-level cold low was closer to the threatened area (southern France), and the region was located just downstream

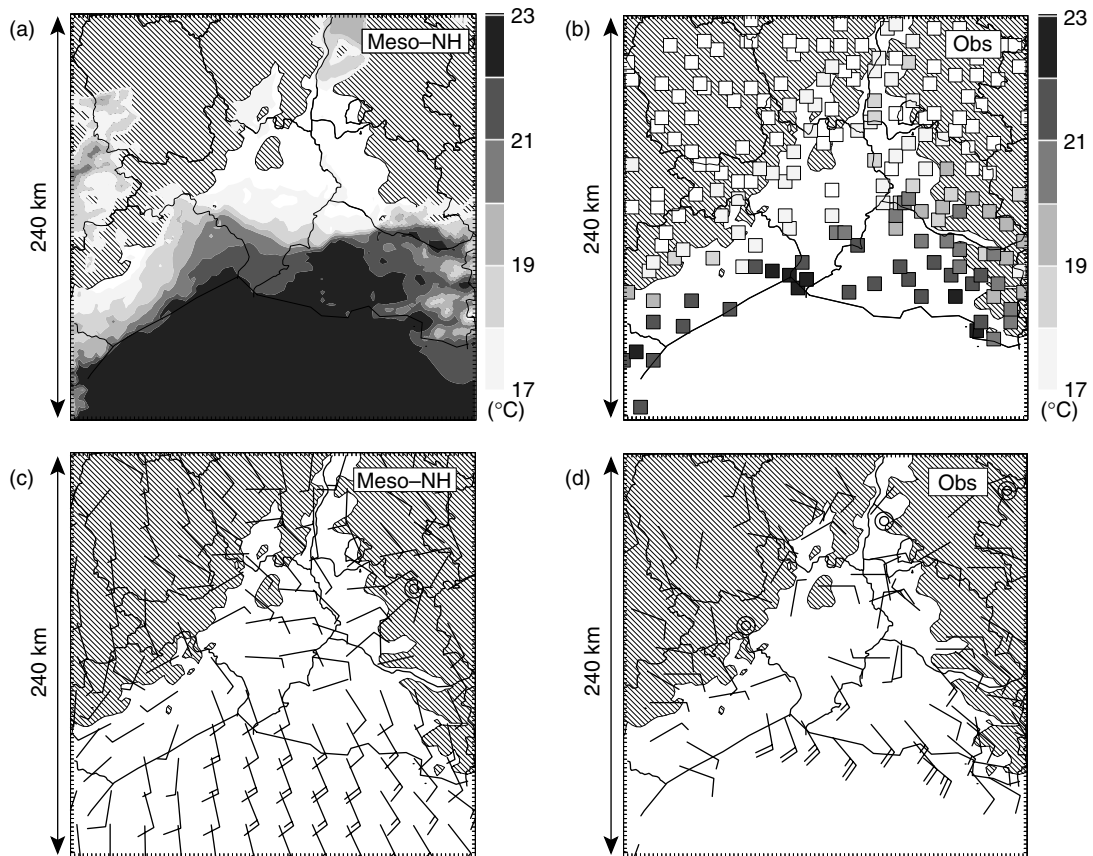


Figure 14. As Figure 10, but for the Gard case. The time is 18 UTC, 8 September 2002.

of the disturbed upper-level ‘jet-streak’. The diffluence associated with the south to southwesterly upper-level flow appeared to be strongest over northern France at 12 UTC on 12 November (Figure 18a). However, at 00 UTC, the trough axis became oriented more north-west–southeast, and southern regions of France become much more directly influenced by the upper-level diffluence. The model also succeeded in simulating fairly well the counterclockwise rotation of the trough axis (Figure 18(b) and (c)) except for later in the simulation when the motion is too fast with respect to the ARPEGE analysis. The fact that the upper-level pattern persisted and lasted through the simulation might generate favourable synoptic conditions for maintenance of convective activity over the area by providing additional upward motion.

4.3.2. Low-level mesoscale environment forecast

The location of the observed very strong low-level flow is well captured by Meso-NH (Figure 19), although the simulated surface winds are slightly weaker than those observed (Figure 19(c) and (d)). The tongue of warmest surface air is well simulated as well as its spatial extent and intensity.

4.3.3. Heavy precipitation forecast

As for the Gard case, the model simulates a precipitating system for the Aude event which is close to the observed

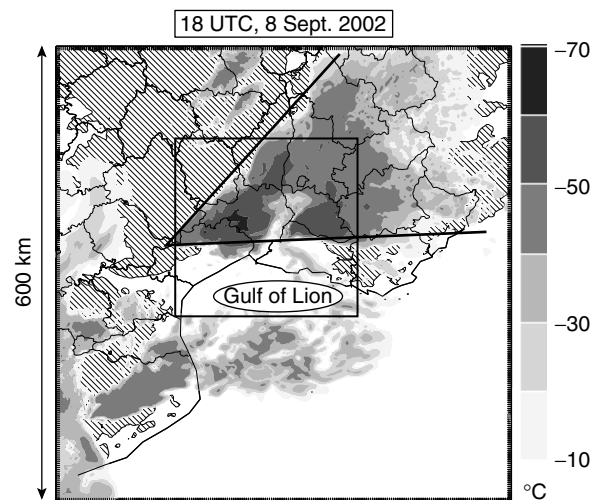


Figure 15. Simulated METEOSAT infrared brightness temperature (shading) for the Gard case from MDA. The bold solid line shows the V-shape of the system at this time and the box represents the subdomain used for Figure 16(a).

one, i.e. a south–north line of precipitation extending from the eastern edge of Pyrenees up to the southwestern part of the Massif Central (Figure 20(a)).

The Aude case is the only one for which Meso-NH is able to trigger a significant precipitation system, even starting from the REF10 simulation. Indeed, Meso-NH already succeeds fairly well in forecasting the

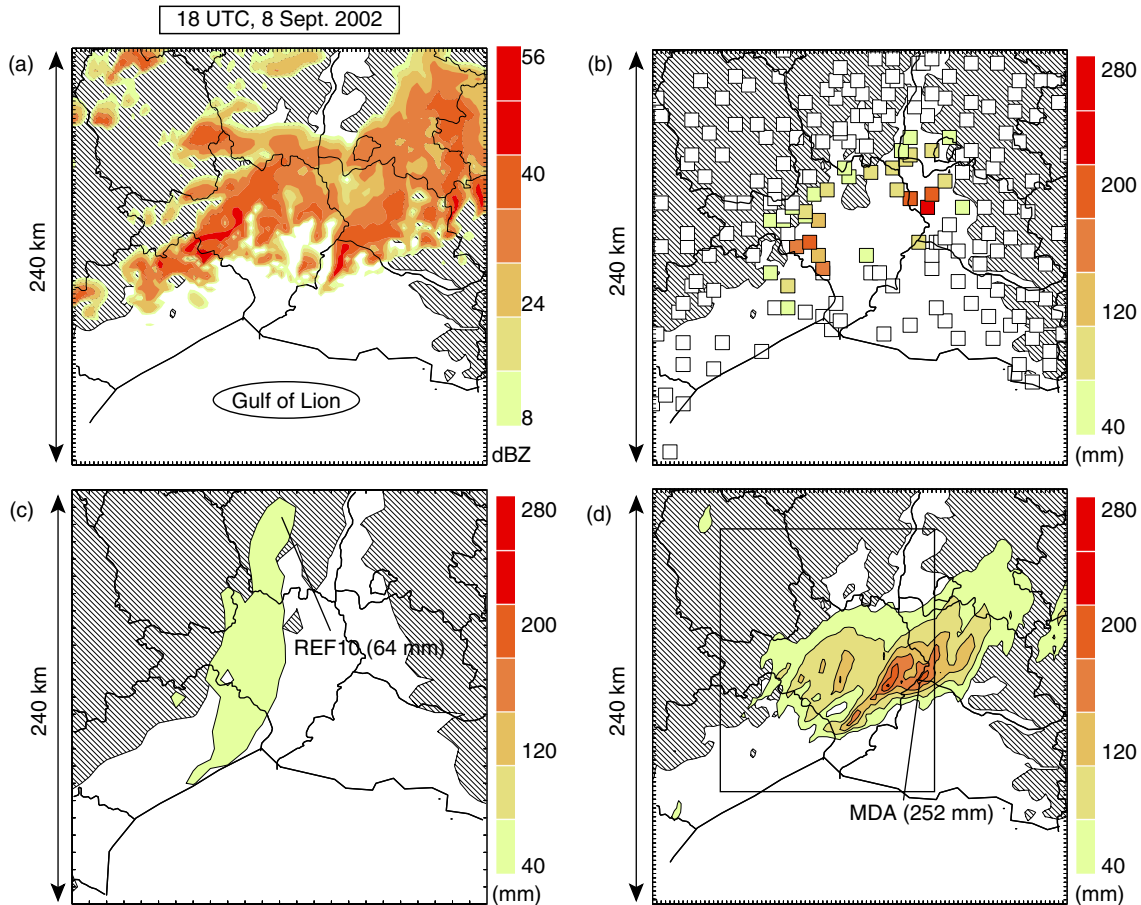


Figure 16. As Figure 11, but for the Gard case from 12 to 22 UTC, 8 September 2002. This figure is available in colour online at www.interscience.wiley.com/qj

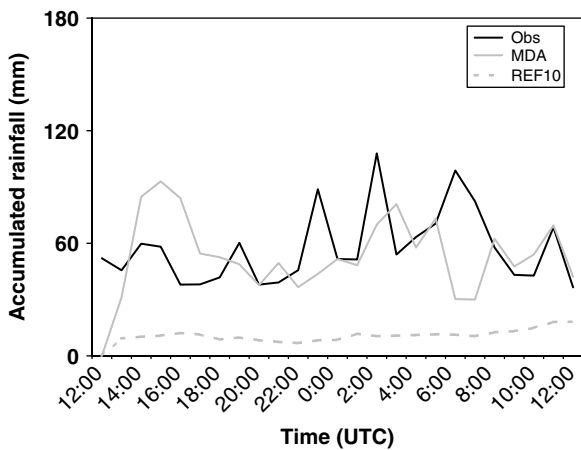


Figure 17. As Figure 12, but for the Gard case within the box shown in Figure 16(d).

location of the heavy precipitation centre over the central eastern region of the Aude department with accumulated rainfall peaking near 210 mm (Figure 20(c)). Increasing the resolution also improves the precipitation forecast with a maximum of 281 mm for the best high-resolution simulation (Figure 20(d)). Moreover, the rainfall time series shown in Figure 21 indicates a strong maximum 1-hour accumulated precipitation of about 50 mm during

the mature stage of the convective system. However, it is important to note that the model produces a slight eastward shift of the area of intense precipitation south of Aude which is weaker than the observations because the simulated trough (as mentioned above) rotates faster than the observed.

For the three cases, it is concluded that Meso-NH succeeds in reproducing realistic structures of the three HPEs since the model captures and correctly simulates the synoptic-scale environment in which the convective systems were embedded.

5. Detailed analysis of synoptic-scale ingredients leading to HPEs

After having evaluated the simulations for the three cases and described the upper-level dynamics favourable for the HPEs, we now emphasize the additional synoptic-scale ingredients that favour long-lasting HPEs. For that purpose, water vapour fluxes at low levels, i.e.

$$\int_{z=0}^{z=3 \text{ km}} \rho_v \mathbf{V}_h dz$$

(where ρ_v is the specific humidity and \mathbf{V}_h the horizontal wind) have been computed at the mature stages of

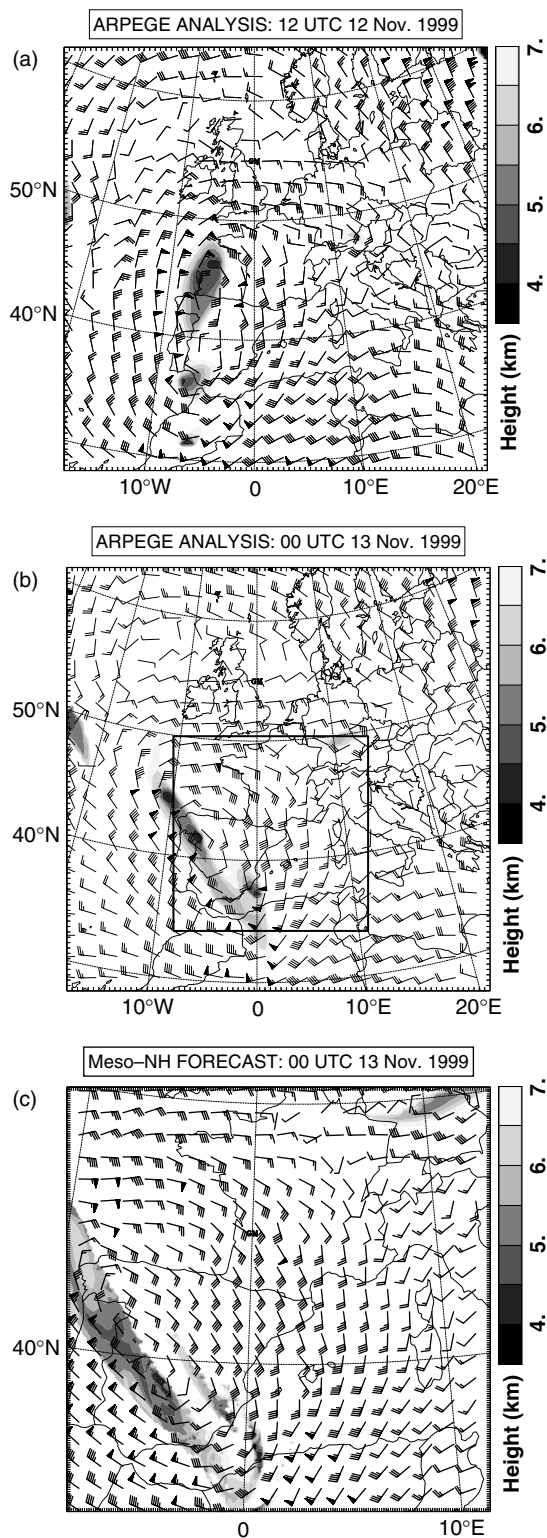


Figure 18. As Figure 9, but for the Aude case.

the convective systems, as well as composites of the simulated conditional convective instability.

5.1. Cévennes case

Figure 22(a) shows the spatial distribution of the simulated convective available potential energy (CAPE) at 1800 UTC on 13 October, i.e. just before the period of

heaviest rain. At this time, significant values of CAPE cover almost the entire western Mediterranean from southeastern France to North Africa (Figure 12(a)). A large area with maximum values greater than 1500 J kg^{-1} is centred just east of the Balearic Islands. Associated with these conditionally unstable air masses over the sea are large amounts of precipitable water (not shown) in the area.

In order to check whether air masses coming from areas of strong conditional convective instability feed the convective area, backward trajectories (Gheusi and Stein, 2002) have been computed. Parcels in the same vertical column as the simulated rainfall maxima (Figures 11, 16 and 20) have been taken at 1.5, 3, 5, 7 and 9 km heights and their origins six hours earlier have been determined. In Figure 22(a), the 6-hour back trajectories from 00 UTC on 14 October are superimposed. The trajectories show that parcels in the area of interest at 00 UTC were over the Mediterranean six hours earlier in the moist and strongly conditionally unstable area discussed above. This result confirms that the tongue of strong CAPE is important for feeding and sustaining the convective activity associated with the Cévennes event. Only the backward trajectory of the parcel at 1.5 km at 00 UTC departs slightly from the others, because of a more southerly flow at low levels. Trajectories are relatively short during the considered 6-hour period due to a slow and almost unidirectional mid- to upper-level flow.

Figure 22(b) reveals a tongue of significant values of water vapour flux coming from the south of Sardinia and from the Balearic Islands which reinforce the idea that, between 12 and 00 UTC, the air coming from the moist and conditionally unstable area mentioned above helps to maintain the convective activity by continuously advecting warm and moist air masses just off the French southeastern coast. It must be also stressed that this low-level synoptic pattern has more or less the same trend in the upper troposphere, i.e. the patterns evolve slowly.

5.2. Gard case

The synoptic environment for the Gard event has some similarities with the Cévennes event in terms of the distribution of the conditional convective instability. At 1800 UTC on 8 September, the atmosphere is quite conditionally unstable and the CAPE field is similar to that for the Cévennes episode, with the largest values (about 1600 J kg^{-1}) located over the northwestern Mediterranean. An interesting pattern shown by the 6-hour back trajectories from 00 UTC (Figure 23(a)) is a significant veering to the southwest with altitude. Indeed, the LLJ contributes to enhance moisture advection whereas the strong mid- to upper-level flow favours northward motion of precipitation out of the triggering area. Such a wind profile is one of the factors which could maintain the rainfall activity. Moreover, as was the case for the Cévennes event, the parcels originate from the moist humid and conditionally unstable regions of the western Mediterranean (Figure 23(a)).

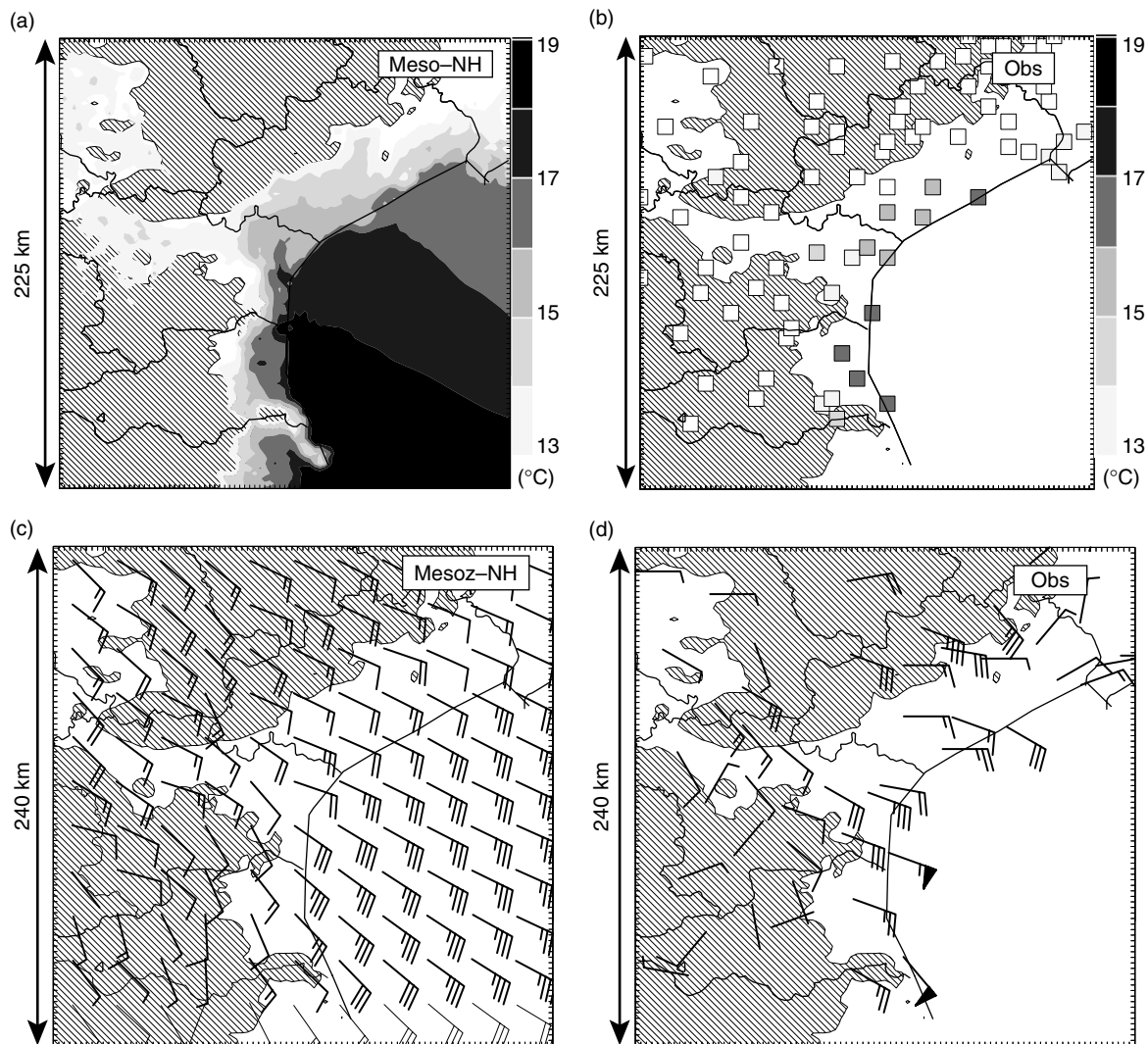


Figure 19. As Figure 10, but for the Aude case at 21 UTC, 12 November 1999.

Strong forcing also prevails at the surface for the Gard event. Indeed, as the cold front progresses slowly eastwards, the water vapour flux in the lower troposphere is increased ahead of the front with strong convergence of the flux upstream of the Rhône valley, bringing more moisture in to feed the convection in the region (Figure 23(b)). Once more, the slow approach of the cold front was a positive factor for advecting high humidity which was necessary to maintain the high precipitation rates over several hours.

5.3. Aude case

Finally, in contrast to the Cévenne and Gard cases, the Aude event has much weaker available conditional convective instability over the Mediterranean Sea. At 18 UTC on 12 November, the strongest values of CAPE (up to 1500 J kg^{-1}) are located near Sardinia, i.e. away from the area of convection (Figure 24(a)).

Nevertheless, the Aude case also exhibits very pronounced low-level forcing in addition to a strong upper-level dynamic circulation already discussed in the previous section. Figure 24(b) depicts a large low-level area

of low pressure centred over the Sierra Nevada (Spain) and an anticyclone over the Italian Alps. Between these structures, a south to southeasterly jet prevails generating a very strong low-level water vapour flux of about $650 \text{ kg s}^{-1}\text{m}^{-2}$ in the 12 hours from 12 UTC on 12 November. On the eastern side of the low, significant northward advection of warm and moist air is probably supported by the strong low-level convergence of the moisture flux which maintains convective activity over the Aude department. As with the previous cases, the low-level synoptic pattern for the Aude event evolves very slowly as the low pressure area over Spain is nearly stationary over at least 12 hours.

6. Summary and concluding remarks

A description of three deep moist convective events which produced floods over southern France has been presented in this first of two linked papers. These particular cases have been selected due to their location over the southern Massif Central foothills, which is a region statistically favoured for very heavy precipitation events.

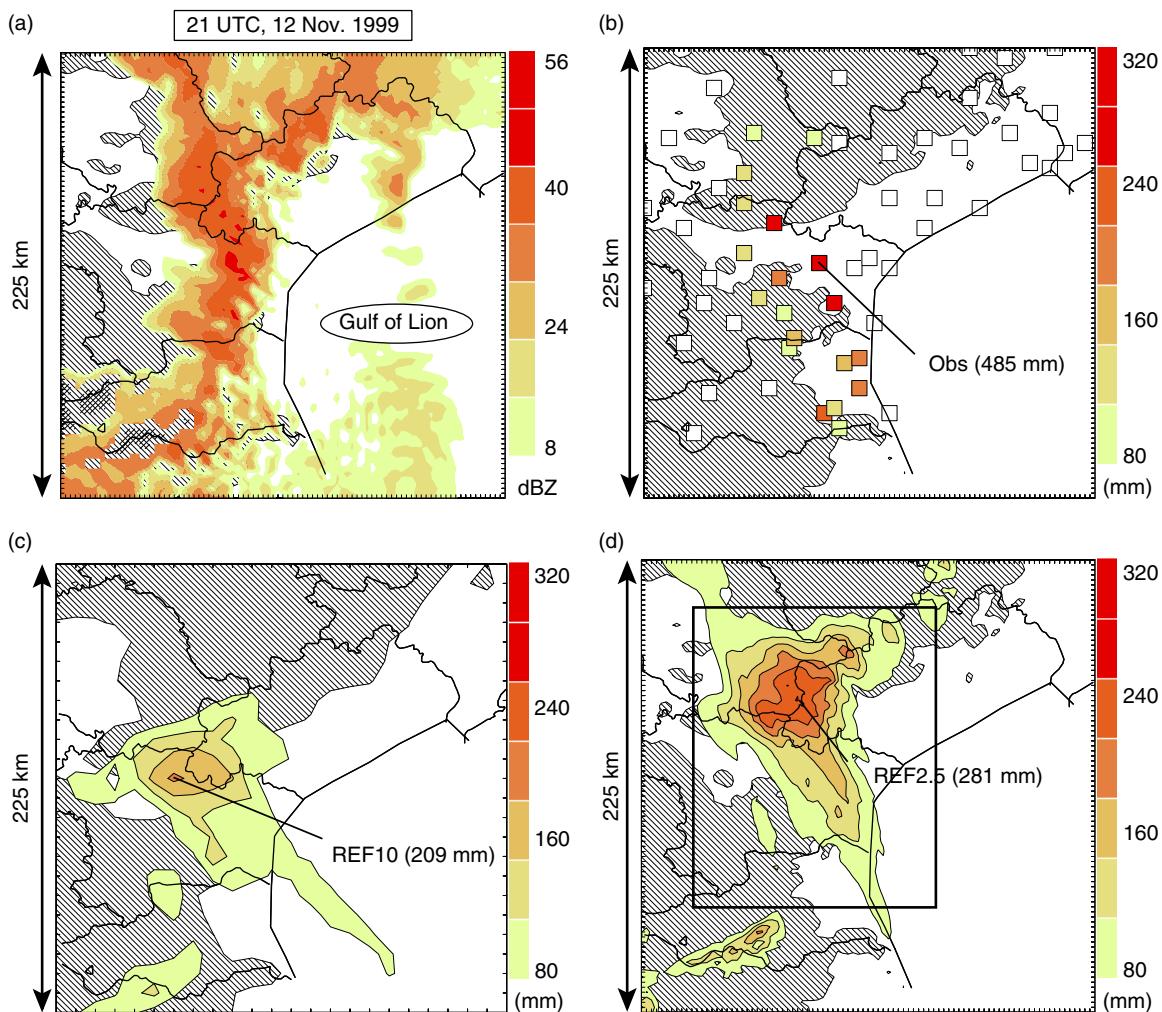


Figure 20. As Figure 11, but for the Aude case from 12 UTC, 12 November to 06 UTC, 13 November 1999. This figure is available in colour online at www.interscience.wiley.com/qj

The aim of the first part of this study was to validate the best high-resolution simulations by comparing some features and the evolution from Meso-NH with the available observations. Moreover, the different synoptic ingredients which favoured the development of quasi-stationary MCSs in the case-studies have also been identified.

These numerical experiments have shown that, first, Meso-NH can reproduce and forecast significant rainfall amounts associated with convective systems with quasi-stationary behaviour (i.e. lasting several hours at the same location). Moreover, the model reproduces fairly well the low-level mesoscale environments associated with the three HPEs. Second, the meteorological synoptic-scale context was analyzed and the evolution in which each convective system was embedded was described. At the synoptic scale, the meteorological patterns for the Gard and the Aude cases were characterized by deep cyclonic circulations generating a strong diffluent southerly flow over the Mediterranean, from the North African coast to France. This upper cold low was initially to the west or to the north-west of France and moved very slowly. For the Cévennes case, although the synoptic forcing was less pronounced, a short-wave trough located off the

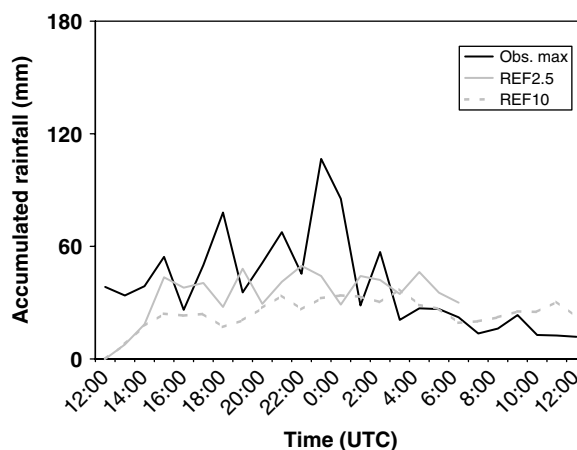


Figure 21. As Figure 12, but for the Aude case within the box shown in Figure 20(d).

North African coast most likely favoured triggering of the convection. For this last case, the synoptic conditions evolved very slowly due to a blocking high located over central Europe. The surface pattern also revealed strong forcing consisting of an anticyclone over the northern

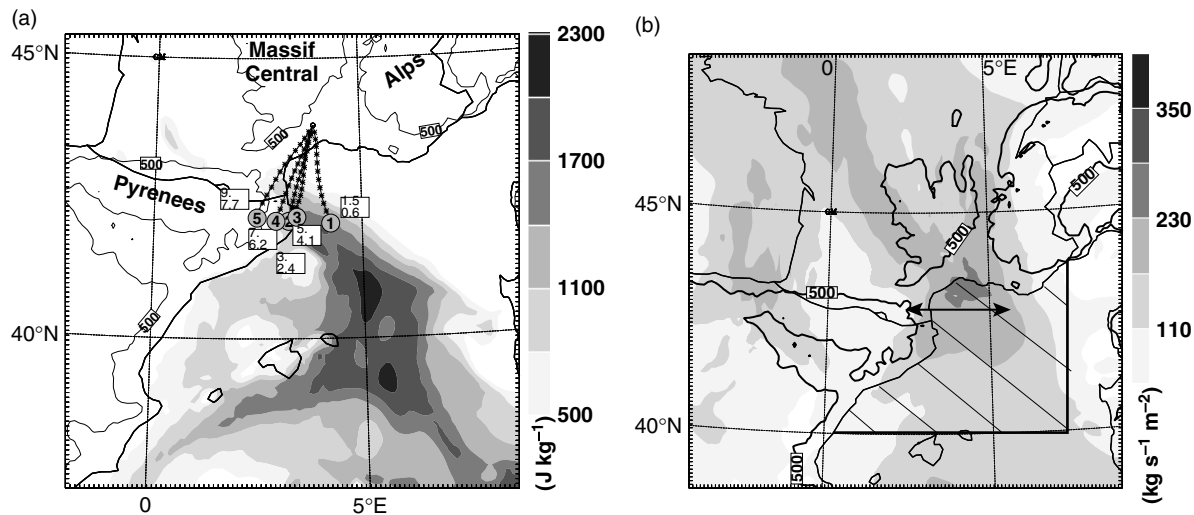


Figure 22. Low-level conducive ingredients for the best simulation for the Cévennes case: (a) simulated CAPE (shading) at 18 UTC, 13 October and (b) water vapour flux (shading) integrated between the surface and 3 km altitude, at 00 UTC, 14 October. (a) also shows 6-hour back trajectories for Lagrangian parcels starting at 00 UTC on 14 October at five heights. Lower and upper boxed labels indicate the height (km) over the flooding area at 00 UTC and at the source regions 6 hours earlier, respectively, and stars mark the parcel positions every 30 minutes. In (b), the hatched box represents the sea area over which CAPE was averaged for Figure 25, and the double-headed arrow denotes the line across which water vapour fluxes were integrated (also for Figure 25) through an area of 280 km length and 3 km height, about 70 km upstream of the flooding area. The 500 m topography contour is shown in both panels.

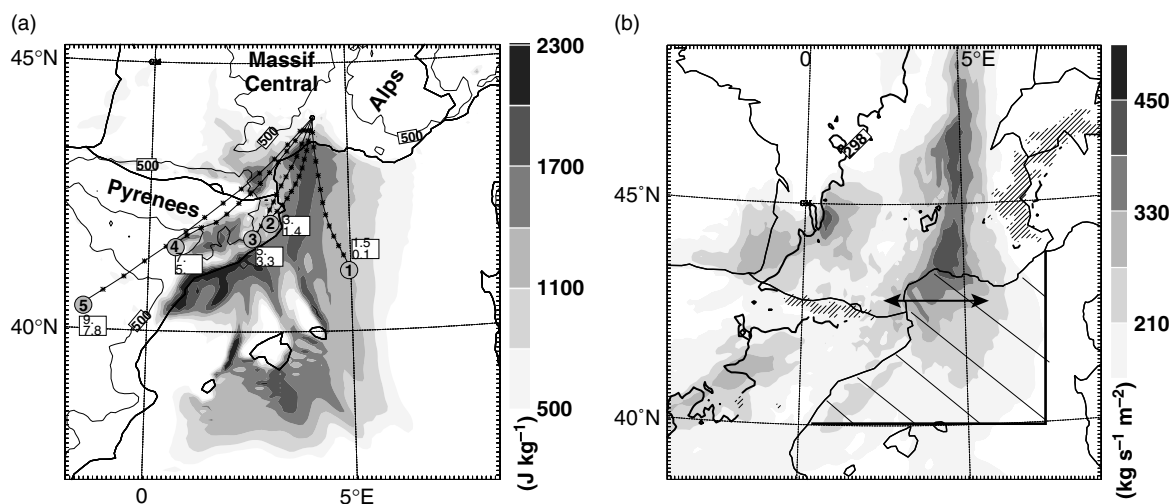


Figure 23. As Figure 22, but for the best simulation for the Gard case. Time is (a) 18 UTC, 8 September and (b) 00 UTC, 9 September. Back trajectories start at 00 UTC, 9 September 2002. The bold contour in (b) denotes virtual temperature of 298 K.

Alps and a low pressure area over Spain for the Aude case, and a slow-moving surface cold front approaching the region for the Gard case. These low-level synoptic patterns induced an intense south to easterly LLJ which favoured strong low-level moisture transport and significant conditional convective instability over the flooded areas. For both extreme HPEs (i.e. Gard and Aude), the main basic ingredients for a flash-flood-producing system, as pointed out by Lin *et al.* (2001) for instance, were present to more or less the same extent for these cases: a conditionally unstable atmosphere and moist low levels in the presence of the large-scale forcing mentioned above and mesoscale lifting (i.e. orographic forcing and low-level convergence). Moreover, low-level moisture

fluxes or CAPE had larger values than those of the more classical heavy rain event (i.e. typical Cévennes cases). The conditional convective instability was weak for the Aude case but seems to be counterbalanced by large moisture fluxes (and *vice versa* for the Gard case), as can be seen in Figure 25. These slow-evolving synoptic ingredients favoured long-lasting rain over southern France in the numerical model.

However, even though synoptic-scale ingredients (upper-level PV anomalies, strong low-level moisture advection, CAPE, etc.) can provide the necessary ingredients for the convective activity, other important mesoscale factors and/or finer-scale processes contribute to continuously focus the activity over the same specific region

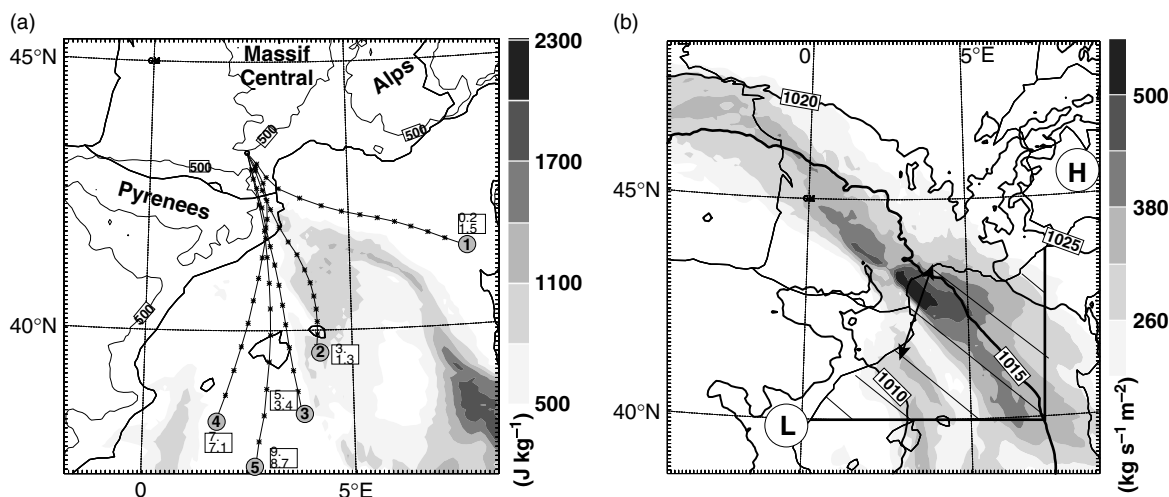


Figure 24. As Figure 22, but for the best simulation for the Aude case. Time is (a) 18 UTC, 12 November and (b) 00 UTC, 13 November 1999. In (b), L and H denote low and high pressure centres; surface isobars (bold) are also shown at 5 hPa intervals.

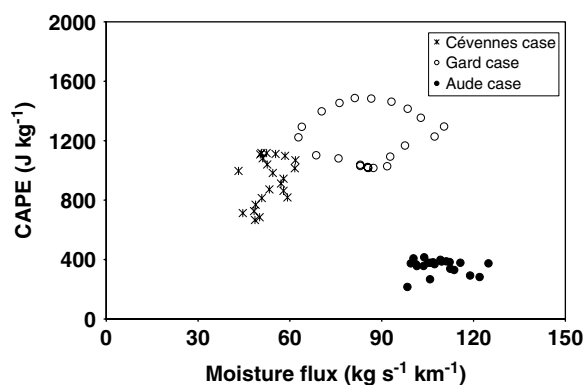


Figure 25. CAPE (J kg^{-1}) versus water vapour flux ($\text{kg s}^{-1} \text{km}^{-1}$) at times through each of the three cases. Both quantities are averaged as indicated in Figure 22.

(the necessary forced ascent to trigger and/or maintain the convection). This paper was dedicated to the evaluation of the best numerical simulation and also the identification of the synoptic-scale ingredients conducive for three flash-flood events over southern France. This, however, is not enough to explain, for instance, why heavy precipitation was located over the plain for the Gard case, i.e. about 80 km southeast of the most statistically favoured region for very heavy precipitation. Based on the best high-resolution numerical experiments with the Meso-NH model, the physical mechanisms leading to the stationarity of the three heavy precipitating systems over a specific region of southern France will be examined and discussed in a companion paper.

Acknowledgements

This work has been carried out in the framework of the FLOODsite project, funding by the EU Sixth Framework Program. We thank A. Boone for improving the English of the manuscript. We gratefully acknowledge the comments made by the anonymous reviewers that helped to significantly improve the quality of the paper.

References

- Bechtold P, Bazile E, Guichard F, Mascart P, Richard E. 2001. A mass-flux convection scheme for regional and global models. *Q. J. R. Meteorol. Soc.* **127**: 869–886.
- Beven KJ, Kirby MJ. 1979. A physically based, variable contributing area model of basin hydrology. *Hydrol. Sci. Bull.* **24**: 43–69.
- Beven KJ, Lamb R, Quinn P, Romanowicz R, Freer J. 1995. *Models of watersheds hydrology*. Water Resources Publications: Colorado, USA.
- Bluestein HB, Jain MH. 1985. Formation of mesoscale lines of precipitation: Severe squall lines in Oklahoma during the spring. *J. Atmos. Sci.* **42**: 1711–1732.
- Bougeault P, Binder P, Buzzi A, Dirks R, Houze R, Kuettner J, Smith RB, Steinacker R, Volkert H. 2001. The MAP Special Observing Period. *Bull. Am. Meteorol. Soc.* **82**: 433–460.
- Bougeault P, Lacarrère P. 1989. Parameterization of orography-induced turbulence in a meso-beta-scale model. *Mon. Weather Rev.* **117**: 1870–1888.
- Brenot H, Ducrocq V, Walpersdorf A, Champollion C, Caumont O. 2006. GPS zenith delay sensitivity evaluated from high-resolution numerical weather prediction simulations of the 8–9 September 2002 flash flood over southeastern France. *J. Geophys. Res.* **111**(D15105): DOI: 10.1029/2004JD005726.
- Buzzi A, Tartaglione N, Malguzzi P. 1998. Numerical simulations of the 1994 Piedmont flood: Role of orography and moist processes. *Mon. Weather Rev.* **126**: 2369–2383.
- Caniaux G, Redelsperger JL, Lafore JP. 1994. A numerical study of the stratiform region of a fast-moving squall line. Part I: General description and water and heat budgets. *J. Atmos. Sci.* **51**: 2046–2074.
- Caumont O, Ducrocq V, Delrieu G, Gosset M, Pinty J-P, Parent du Châtelet J, Andrieu H, Lemaître Y, Scialom G. 2006. A radar simulator for high-resolution non-hydrostatic models. *J. Atmos. Oceanic Technol.* **20**: 1049–1067.
- Chancibault K, Anquetin S, Ducrocq V, Saulnier G-M. 2006. Hydrological evaluation of high resolution precipitation forecasts of the Gard flash-flood event (8–9 September 2002). *Q. J. R. Meteorol. Soc.* **132**: 1091–1117.
- Chappell CF. 1986. Quasi-stationary convective events. Pp 289–310 in *Mesoscale meteorology and forecasting*. Ray PS (ed). Amer. Meteorol. Soc: Boston.
- Clark TL, Farley RD. 1984. Severe downslope windstorm calculations in two and three spatial dimensions using anelastic interactive grid nesting: A possible mechanism for gustiness. *J. Atmos. Sci.* **41**: 329–350.
- Cuxart J, Bougeault P, Redelsperger J-L. 2000. A turbulence scheme allowing for mesoscale and large-eddy simulations. *Q. J. R. Meteorol. Soc.* **126**: 1–30.
- Delrieu G, Ducrocq V, Gaume E, Nicol J, Payrastré O, Yates E, Kirstetter P-E, Andrieu H, Ayrat P-A, Bouvier C, Creutin J-D, Livet M, Anquetin S, Lang M, Neppel L, Obled C, Parent-du-Châtelet J, Saulnier G-M, Walpersdorf A, Wobrock W. 2005. The

- catastrophic flash-flood event of 8–9 September 2002 in the Gard region, France: A first case-study for the Mediterranean Hydro-meteorological Observatory. *J. Hydrometeorol.* **6**: 34–52.
- Doswell CA III, Ramis C, Romero R, Alonso S. 1998. A diagnostic study of three heavy precipitation episodes in the Western Mediterranean region. *Weather and Forecasting* **13**: 102–124.
- Ducrocq V, Lafore J-P, Redelsperger JL, Orain F. 2000. Initialization of a fine-scale model for convective system prediction: A case-study. *Q. J. R. Meteorol. Soc.* **126**: 3041–3066.
- Ducrocq V, Ricard D, Lafore J-P, Orain F. 2002. Storm-scale numerical rainfall prediction for five precipitating events over France: On the importance of the initial humidity field. *Weather and Forecasting* **17**: 1236–1256.
- Ducrocq V, Alullo G, Santurette P. 2003a. Les précipitations intenses et les inondations du 12 et 13 Novembre 1999 sur le sud de la France. *La Météorologie* 8th série, **42**: 18–27.
- Ducrocq V, Lebeaupin C, Thouvenin T, Giordani H. 2004. L'événement des 8–9 septembre 2002: Situation météorologique et simulation à mésoéchelle. *La Houille Blanche* **6**: 86–92.
- Ferretti R, Low-Nam S, Rotunno R. 2000. Numerical simulations of the Piedmont flood of 4–6 November 1994. *Tellus* **52A**(:): 162–180.
- Fernandez C, Gaertner MA, Gallardo C, Castro M. 1995. Simulation of a long-lived Meso- β scale convective system over the Mediterranean coast of Spain. Part I: Numerical predictability. *Meteorol. Atmos. Phys.* **56**: 157–179.
- Frei C, Shär C. 1998. A precipitation climatology of the Alps from high-resolution raingauge observations. *Int. J. Climatol.* **18**: 873–900.
- Gal-Chen T, Somerville RCJ. 1975. On the use of a coordinate transformation for the solution of the Navier–Stokes equations. *J. Comput. Phys.* **17**: 209–228.
- Gaume E, Livet M, Desbordes M, Villeneuve J-P. 2004. Hydrological analysis of the river Aude, France, flash flood on 12 and 13 November 1999. *J. Hydrol.* **286**: 135–154.
- Gheusi F, Stein J. 2002. Lagrangian description of airflows using Eulerian passive tracers. *Q. J. R. Meteorol. Soc.* **128**: 337–360.
- Hamadache B, Terchi A, Brachemi O. 2002. Study of the meteorological situation which affected the west and the centre of Algeria in general and Bab-el-oued in particular on 10 November 2001. Proceedings of fourth EGS Plinius Conference, Mallorca, Spain, CD-ROM.
- Hernandez E, Cana L, Diaz J, Garcia R, Gimeno L. 1998. Mesoscale convective complexes over Western Mediterranean area during 1990–1994. *Meteorol. Atmos. Phys.* **68**: 1–12.
- Homar V, Romero R, Ramis C, Alonso S. 1999. A case of convection development over the Western Mediterranean Sea: A study through numerical simulations. *Meteorol. Atmos. Phys.* **71**: 169–188.
- Huet P, Martin X, Prime J-L, Foin P, Laurain C, Cannard P. 2003. 'Retour d'expérience des crues de Septembre 2002 dans les départements du Gard, de l'Hérault, du Vaucluse, des Bouches-du-Rhône, de l'Ardèche et de la Drôme'. Technical report, Ministère de l'écologie et du développement durable: Paris, France.
- Jansa A, Genoves A, Angeles Picornell M, Campins J, Riosalido R, Carretero O. 2001. Western Mediterranean cyclones and heavy rain. Part 2: Statistical approach. *Meteorol. Appl.* **8**: 43–56.
- Kain JS, Fritsch JM. 1990. A one-dimensional entraining/detraining plume model and its application in convective parameterizations. *J. Atmos. Sci.* **47**: 2784–2802.
- Kain JS, Fritsch JM. 1993. Convective parameterization for mesoscale models: the Kain–Fritsch scheme. *Meteorol. Monogr.* **46**: 165–170.
- Lafore J-P, Stein J, Ascencio N, Bougeault P, Ducrocq V, Duron J, Fisher C, Hereil P, Mascart P, Pinty J-P, Redelsperger J-L, Richard E, Vila-Guerau de Arellano J. 1998. The Meso-NH Atmospheric Simulation System. Part I: Adiabatic formulation and control simulations. *Ann. Geophys.* **16**: 90–109.
- Lin Y-L, Chiao S, Wang T-A, Kaplan ML, Weglarz RP. 2001. Some common ingredients for heavy orographic rainfall. *Weather and Forecasting* **16**: 633–659.
- Llasat MC, Puigcerver M. 1994. Meteorological factors associated with floods in the North-eastern part of the Iberian Peninsula. *Nat. Hazards* **9**: 81–93.
- Maddox R-A, Chapell C-F, Hoxit L-R. 1979. Synoptic and meso-alpha scale aspects of flash flood events. *Bull. Am. Meteorol. Soc.* **60**: 115–123.
- Massad AC, Wernli H, Davies HC. 1998. Heavy precipitation on the Alpine south side: An upper-level precursor. *Geophys. Res. Lett.* **25**: 1435–1438.
- Penarrocha D, Estrela M, Millan M. 2002. Classification of daily rainfall patterns in a Mediterranean area with extreme intensity levels: the Valencia region. *Int. J. Climatol.* **22**: 677–695.
- Pinty J-P, Jabouille P. 1998. A mixed-phased cloud parameterization for use in a mesoscale non-hydrostatic model: Simulations of a squall line and orographic precipitation. Pp 217–220 in Preprints, Conference on Cloud Physics, Everett, WA. Amer. Meteorol. Soc: Boston.
- Redelsperger J-L, Sommeria G. 1981. Méthode de représentation de la turbulence d'échelle inférieure à la maille pour un modèle tridimensionnel de convection nuageuse. *Boundary-Layer Meteorol.* **21**: 509–531.
- Ricard D. 2005. Modélisation à haute résolution des pluies intenses dans les Cévennes: Le système convectif des 13 et 14 Octobre 1995. *La Météorologie* 8th série, **42**: 28–38.
- Riosalido R. 1990. Characterization of mesoscale convective systems by satellite pictures during PREVIMET MEDITERR-ANEO-89 (In Spanish). Pp. 135–148 in Proc. Segundo Simposio Nacional de Prediccion, Madrid. Available from Instituto Nacional de Meteorologia, Apartado 285, 28071 Madrid, Spain.
- Rivrain J-C. 1997. Les épisodes orageux à précipitations extrêmes sur les régions méditerranéennes de la France. *Phénomènes remarquables* **4**: Météo-France: Toulouse.
- Romero R, Doswell CA III, Ramis C. 2000. Mesoscale numerical study of two cases of long-lived quasi-stationary convective systems over Eastern Spain. *Mon. Weather Rev.* **128**: 3731–3751.
- Rotunno R, Ferretti R. 2001. Mechanisms of intense Alpine rainfall. *J. Atmos. Sci.* **58**: 1732–1749.
- Scofield RA. 1985. 'Satellite convective categories associated with heavy precipitation'. Pp 42–51 of Preprints for Sixth Conference on Hydrometeorology, 29 October 1985, Indianapolis. Amer. Meteorol. Soc: Boston.
- Sénési SP, Bougeault P, Chèze J-L, Cosentino P, Thepenier R. 1996. The Vaison-la Romaine flash flood: Mesoscale analysis and predictability issues. *Weather and Forecasting* **11**: 417–442.
- Stein J, Richard E, Lafore J-P, Pinty J-P, Ascencio N, Cosma S. 2000. Meso-NH simulations with grid-nesting and ice phase parameterization. *Meteorol. Atmos. Phys.* **72**: 203–221.